The Uppermost Nappes of the Asterousia Mountains – from Apesokari to Lentas via Miamou

View of Krotos village. The gravel road descending from the village leads to a valley containing metapelites and their migmatite rocks. On the way there one also encounters "Pindos" limestone and ultramafic slope talus

Compiled by George Lindemann, MSc.

Berlin, August 2024

Content

Appendix

1 Introduction

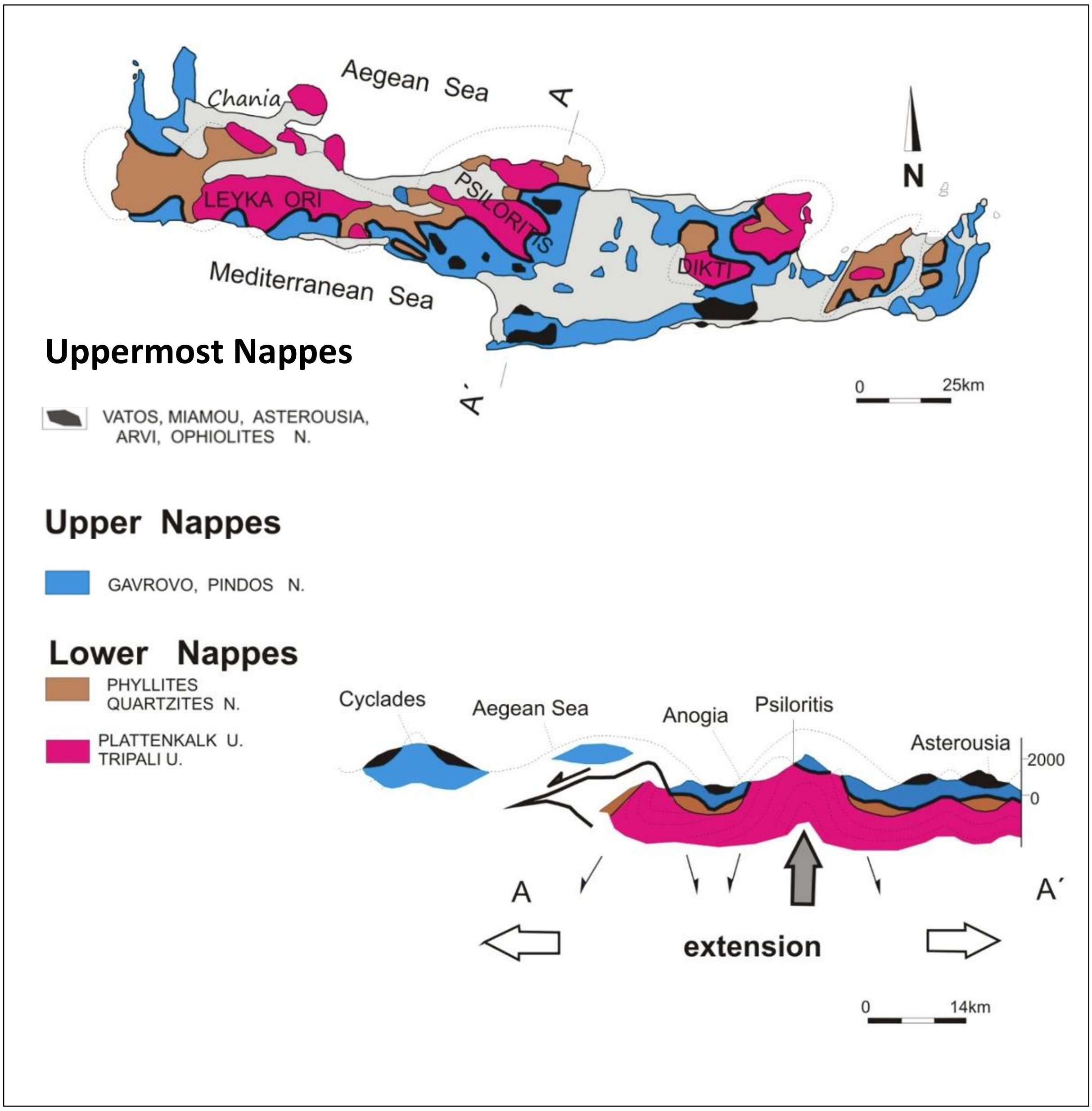

Source: Journal of the virtual explorer (NW Crete, online)
https://virtualexplorer.com.au/article/2011/285/neotectonic-study-of-western-crete/setting.html

A nappe or thrust sheet is a large sheetlike body of rock that has been moved several tens or even hundreds of kilometers along a thrust plane from its original position. Nappes form in convergent tectonic settings such as continental collision zones or on the overriding plate in active subduction zones. The resulting structure may include large-scale recumbent folds, shearing along the fault plane, imbricate thrust stacks, fensters and klippes *[Wikipedia]*.

A characteristic feature of the Uppermost Nappes of southern and central Crete is the frequent occurrence of ophiolites, which represent pieces of oceanic crust predominantly from ocean ridges. Ophiolites consist of mafic to ultramafic plutonic and volcanic rocks and often exhibit deep marine sediments such as clay (i.e. shale, slates and phyllites), chert and deep marine limestones. The ultramafic rock is often hydrothermally altered to serpentinite.

In central Crete, the ophiolite-bearing Uppermost Nappes feature tectonic mélanges that are indicated to be the result of chaotic thrusts within the accretionary wedge of a subduction zone (cf. Cowan, 1985; Hsu, 1968; Raymond, 1984). These assemblages of disrupted rocks represent the highest tectonic nappes overlying the Tripolitza and the Pindos Nappes. *[Tortorici]*

Recent work by Zulauf et. al. 2023 indicates that the Uppermost Nappes can be divided into several separate nappes, based on their lithology and on the grade and timing of metamorphism (e.g. Bonneau, 1972; Krahl, Herbart & Katzenberger, 1982; Tortorici et al. 2012). There are two different stacks one of which is exposed in central Crete and the other in the Asterousia Mountains. The nappe stack in the Asterousia Mountains consists of the Avri, Miamou, "Green Schist" (mostly south of Dikti Mts.) and the Asterousia Crystalline Complex (see also My GeoGuide "No. 22: Uppermost Nappes within the Asterousia Mts.,_Coast Road Kali Limenes to Chrysostoms" concerning the nappes along the coast) *[Zulauf]*.

The Amphibolite facies metamorphic rocks that are intruded by Late Cretaceous granitoid plutonic rocks (Kneuker et al. 2015; Martha et al. 2016, 2017) are referred to as the Asterousia Crystalline Complex (ACC), which is generally regarded to correlate with the southern margin of the Pelagonian domain and therefore lies within the Internal Hellenides (Martha et al. 2017). Other tectonometamorphic nappes ascribed to the Uppermost Unit include the prehnite-pumpellyite facies Arvi Unit, which is interpreted as a Maastrichtian seamount at the northern margin of the Pindos realm (Palamakumbura, Robertson & Dixon, 2013), and the Greenschist Unit, consisting of fine-grained epidote-amphibole schist with a mid-ocean ridge basalt (MORB) -type signature (Reinecke et al. 1982; Martha et al. 2017) *[Martha]*. Note that not all of the nappes are exposed at or near at a single location owing to erosion and young sediment covering.

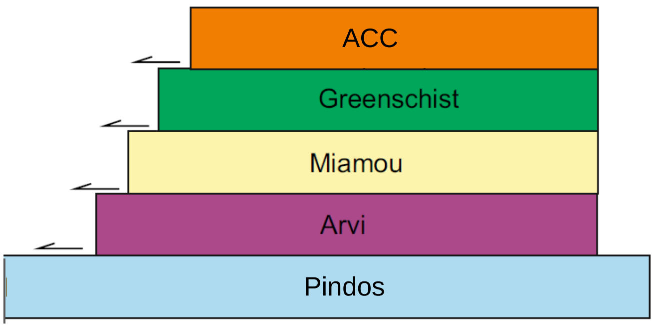

The Uppermost Nappes in the area of the Asteroussia Mountains (Zulauf et. al , 2023)

Unit/nappe Type	Protolith age	Metamorphic facies	Metamorphism Age
ACC	?	Amphibolite-Granulite (2)	Campanian (2, 4, 5)
Greenschist	?	Greenschist (1, 4)	Paleocene (1)
Miamou	Kimmeridgian (15)	Greenschist (15)	?
Arvi	Upper Cretaceous (16, 17)	Prehnite-Pumpellyte (16, 17)	?

(1) Reinecke et al. (1982), (2) Seidel et al. (1976), (3) Seidel et al. (1977), (4) Martha et al. (2017), (5) Martha et al. (2019), (6) Liati et al. (2004), (7) Bonneau and Lys (1978), (8) Zulauf et al. (2023a), (9) Koepke et al. (2002), (10) Malten (2019), (11) Koepke (1986), (12) Koepke et al. (1997), (13) Tortorici et al. (2012), (14) Zulauf et al. in prep., (15) Bonneau et al. (1974), (16) Robert and Bonneau (1982), (17) Palamakumbura et al. (2013), and (18) Karakitzios (1988)

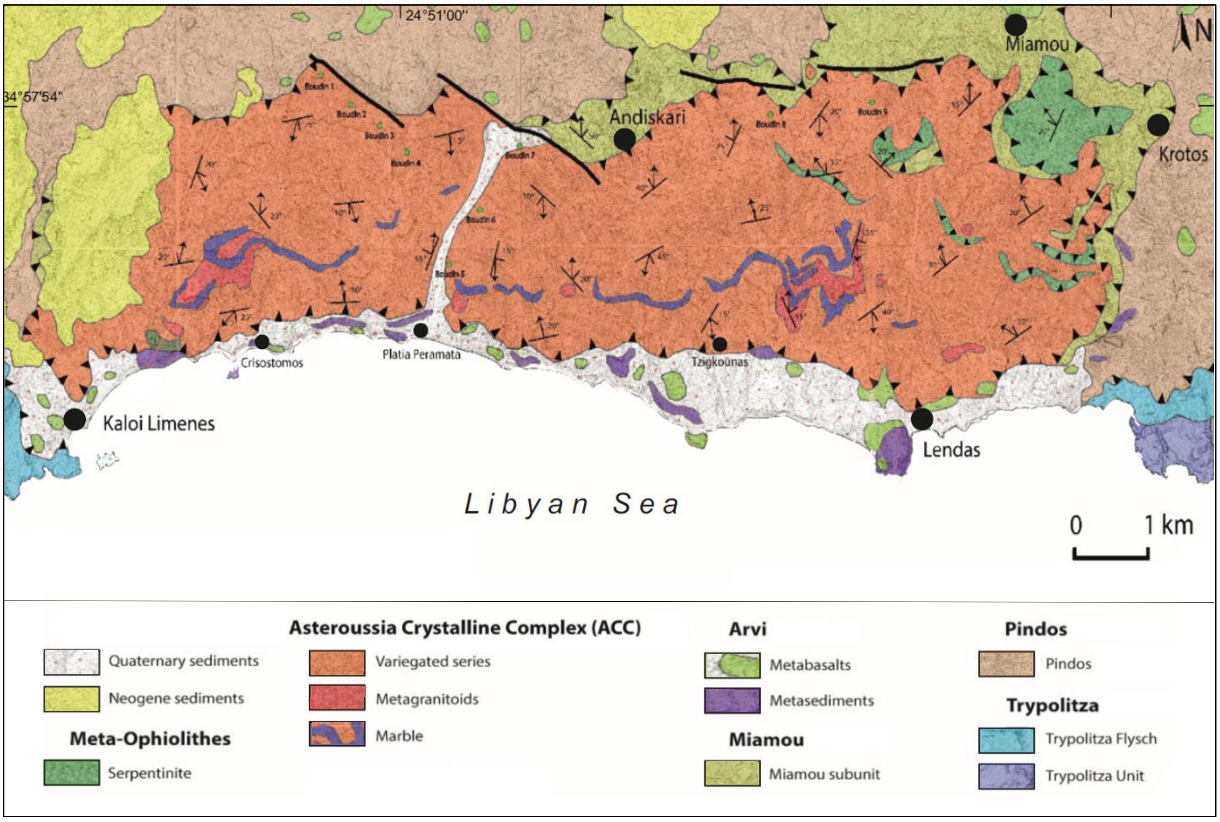

Geological map of the western part of the Asterousia Mountains showing the area between Kaloi Limenes and Lentas. Source: Zulauf G. et al., 2023, (modified after Davi and Bonneau 1972; Thorbecke 1987; Tortorici et al. 2012; Neuwirth 2018).

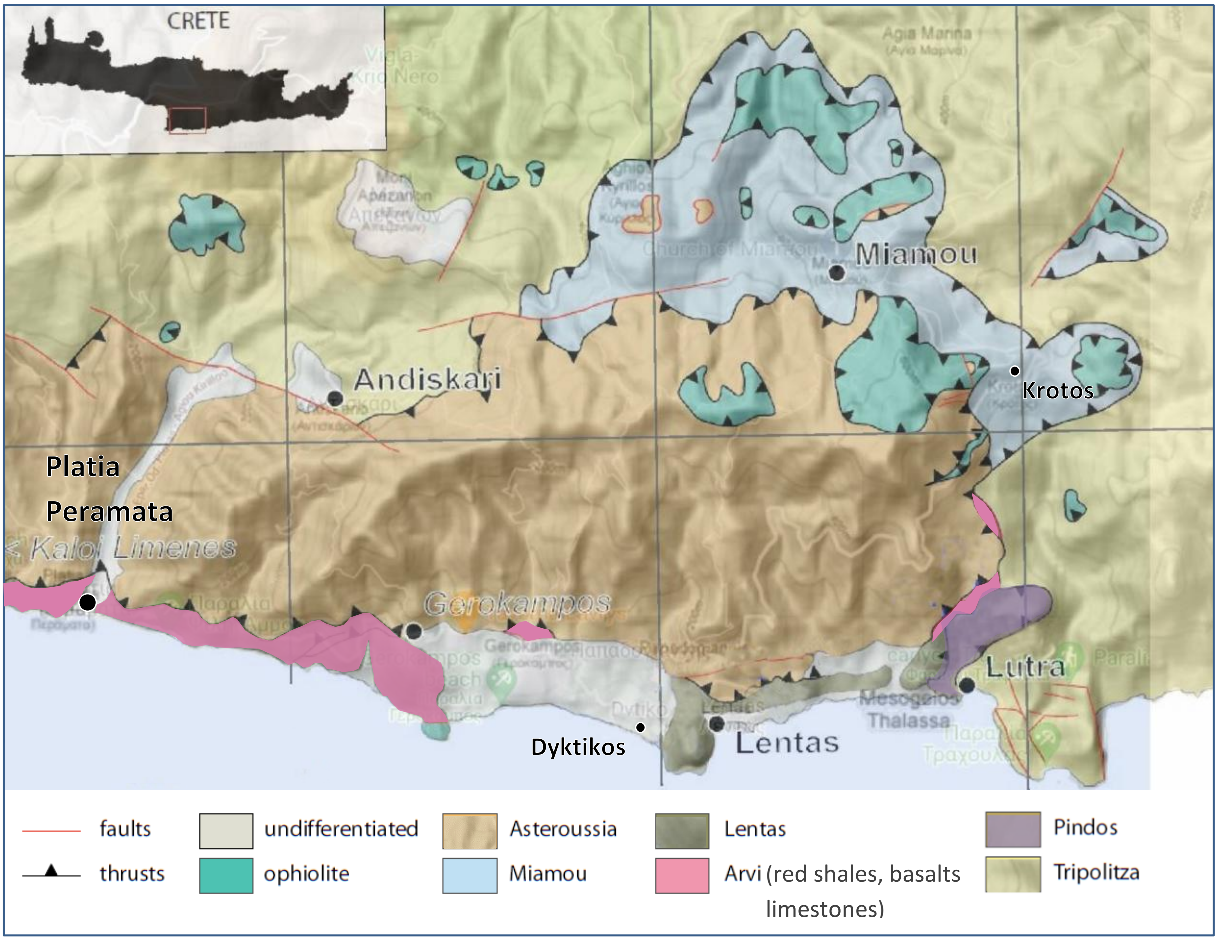

Geological map of the area between Platia Peramata and Luta slightly modified after Champod E. et al., 2010 and Vachard D. et al. 2013: Tectonic map - Andiskarion sheet, modified after Davi & Bonneau (1985) [Stampfli, 2010: Field Course]

2 Apesokari to Miamou

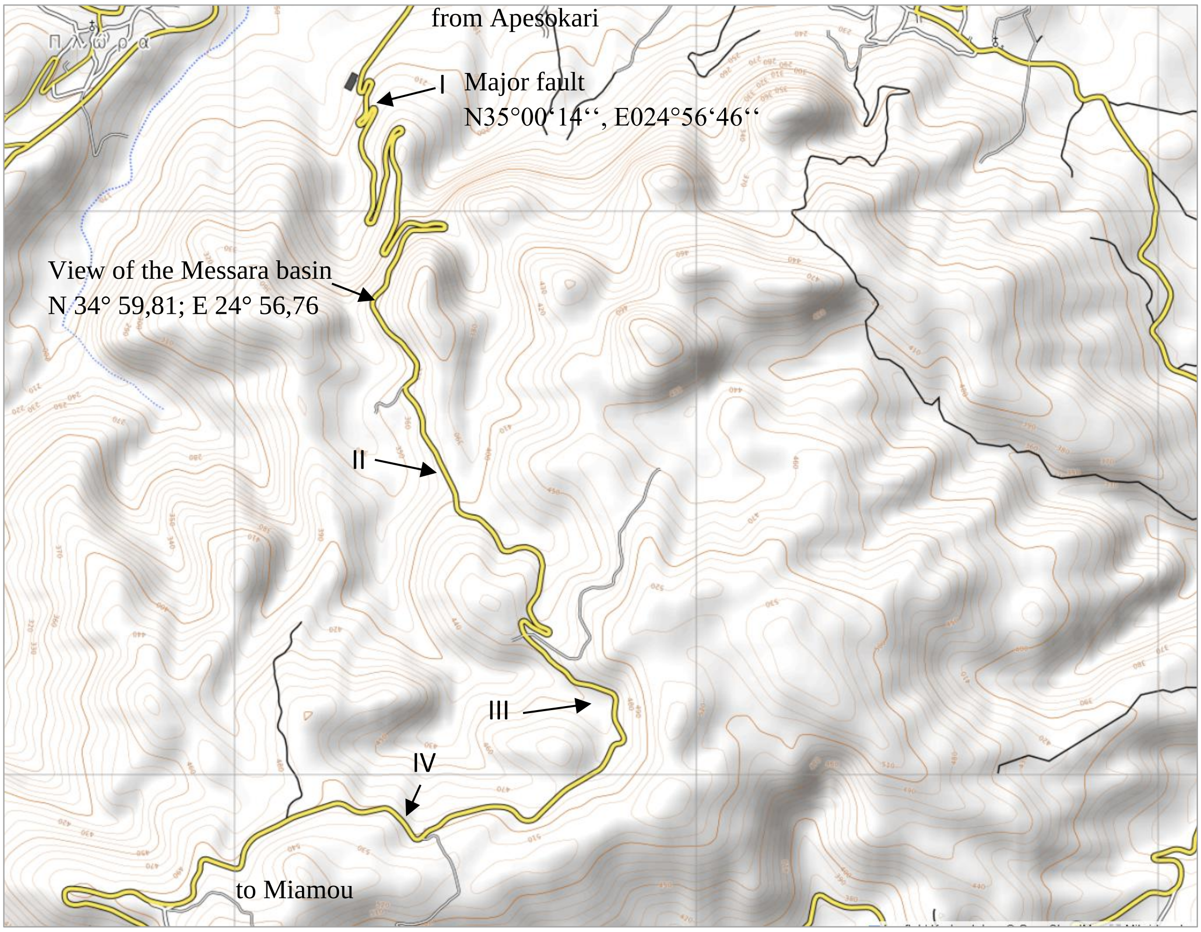

Location of Outcrops

A major normal fault representing the southern boundary of the Messara graben is accessible at the sharp hairpin bend above the village of Apesokari. The west-east striking fault displays the down thrust Neogene limestone rocks of the Ag. Varvara Formation that is offset against Pindos-Flysch (Fassoulas 2000). Along the winding road up the mountain side there are outcrops of the flysch consisting of siltstones and sandstones. Phyllites and individual limestone beds are also exposed within the Pindos flysch displaying intensive tectonic deformation resulting from compressional stress during the Oligocene. Embedded within the flysch are large blocks of Tripoliza limestone, which have been exposed by erosion of the much softer flysch and form cliffs and ridges. Owing to compressional forces the limestone blocks were broken off and incorporated into the flysch. The limestone blocks are regarded by some to be olistholites – a prosses involving submarine gravity sliding. At the chapel of Ag. Marina, Tripoliza limestones with nummulites and rudists have been found.

Above the winding road there is a car park (N 34° 59.81; E 24° 56.76) from which there is a good view of the Messara basin / graben. In the distance are the Psiloritis Mountains that represent an anticlinorium. The foothills are reported to be staggered Neogene tectonic blocks, which were created during the extension of the Messara graben *[Kull U., 2012]*.

Outcrop I. Major normal fault bordering the southern edge of the Messara basin. 1: Neogene shallow marine limestone (Varvara Formation), 2: Tripoliza flysch, 3: Fault zone

Outcrop I. Tripoliza flysch consisting of silty phyllite

Outcrop I. Neogene limestone 1: red algae, 2: presumably reworked coral

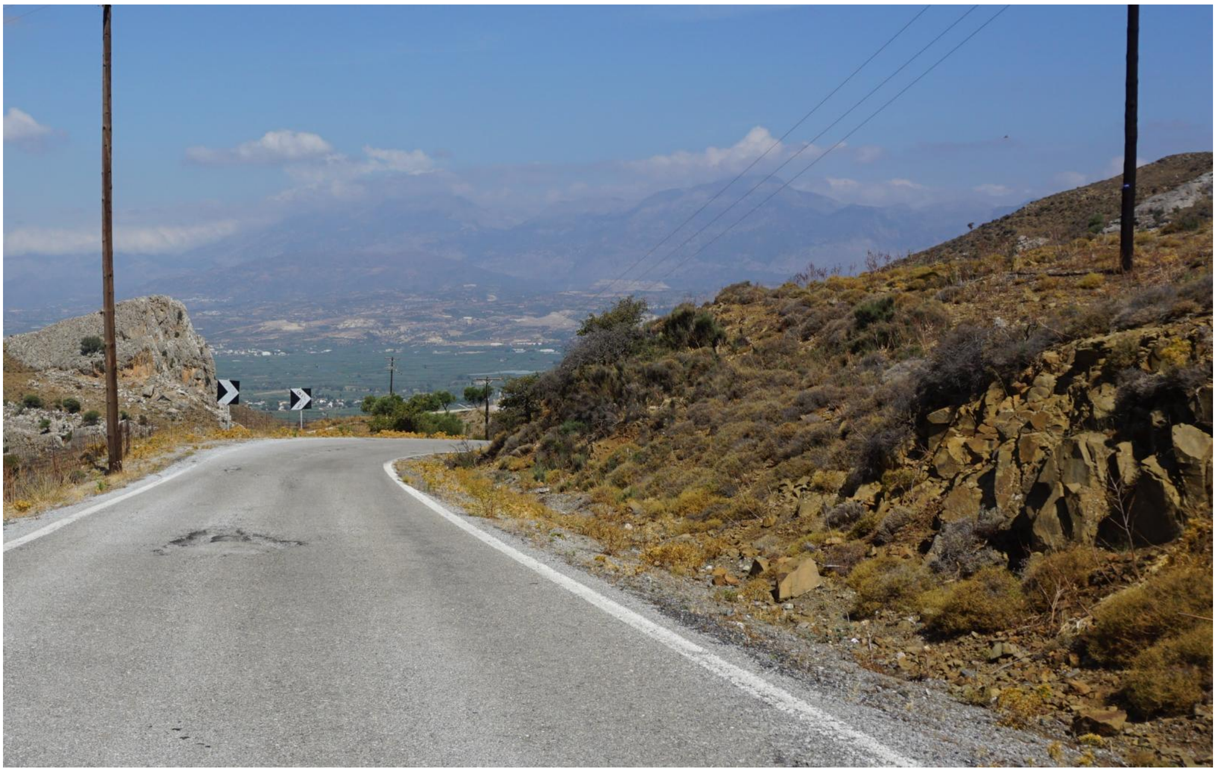

Outcrop II, View of the road leading to carpark looking North. In the background view of the Messara basin.

Outcrop II, Tripoliza flysch consisting of phyllite and sandstone beds

Outcrop II, closeup of previous picture showing fine grained silty sandstone

Outcrop III, 1: Pindos flysch, 2: Isolated limestone block surrounded by flysch thought to be a olistholite. Olistholites are fragments of rock or a rock sequence that are usually angular shaped, quite large and are intercalated in flysch. They are part of an Olisthostrome that arises from submarine sliding of unstable masses. Olisthostromes are characterized by a chaotic mixture of unstratified sediments sometimes several hundreds of metres thick.

Outcrop IV. View looking eastwards. Hilly flysch landscape displaying limestone cliffs and ridges. 1: Slope talus, 2: Limestone block shown on previous picture. It is thought to be the remains of a former *limestone shelf. The blocks (sometimes hundreds of meters large) that are intercalated within flysch are referred to as blocky flysch [Thomson S. N., 1998]*

Outcrop IV. 1: Limestone/ marble boulder (talus) containing red chert, 2: Flysch.

Outcrop IV. Red chert reminiscent of the deep marine Pindos facies. When scratched with a hardened steel nail, a trail of steel is left behind, indicating it to be quite hard (> Mohs scale 7). Deep marine *chert often consists radiolarite, a form of plankton that produces silica tests. When dead they sink to the ocean bed and form a type silica gel, which eventually becomes rock during diageneses.*

Outcrop IV. Sample from a different boulder embedded in flysch. It consists of inhomogeneous grey limestone with different limestone clasts (arrow).

3 Miamou to Krotos

3.1 Miamou Nappe

The Miamou Unit consists of flyschoid terrigenous sediments, diabase and limestones. These rocks underwent greenschist-facies metamorphism. The flyschoid metasedimentary rocks (pelites, sandstones) are intercalated by shallow marine limestone lenses of Late Jurassic age (probably Kimmeridgian). According to Martha et al. (2017, 2019) the flyschoid metasedimentary nappe is of Paleocene age, displays greenschist-facies and underwent top-to-the SE displacement, which is also documented at a number of other locations on Crete (i.e. Melambes and Pefkos areas). Owing to the presents of mafic and ultramafic rocks and the chaotic structure attributed to gravity sliding the Miamou Unit is referred to by some as an ophiolitic nappe.

3.2 Ophiolites

An ophiolite is a section of the Earth's oceanic crust and the underlying upper mantle that has been uplifted and exposed above sea level and often emplaced onto continental crustal rocks. Their great significance relates to their occurrence within mountain belts such as the Alps and Himalayas, and Hellinides where they document the existence of former ocean basins that have now been consumed by subduction. This insight was one of the founding pillars of plate tectonics, and ophiolites have always played a central role in plate tectonic theory and the interpretation of ancient mountain belts. *[Wikipedia]*

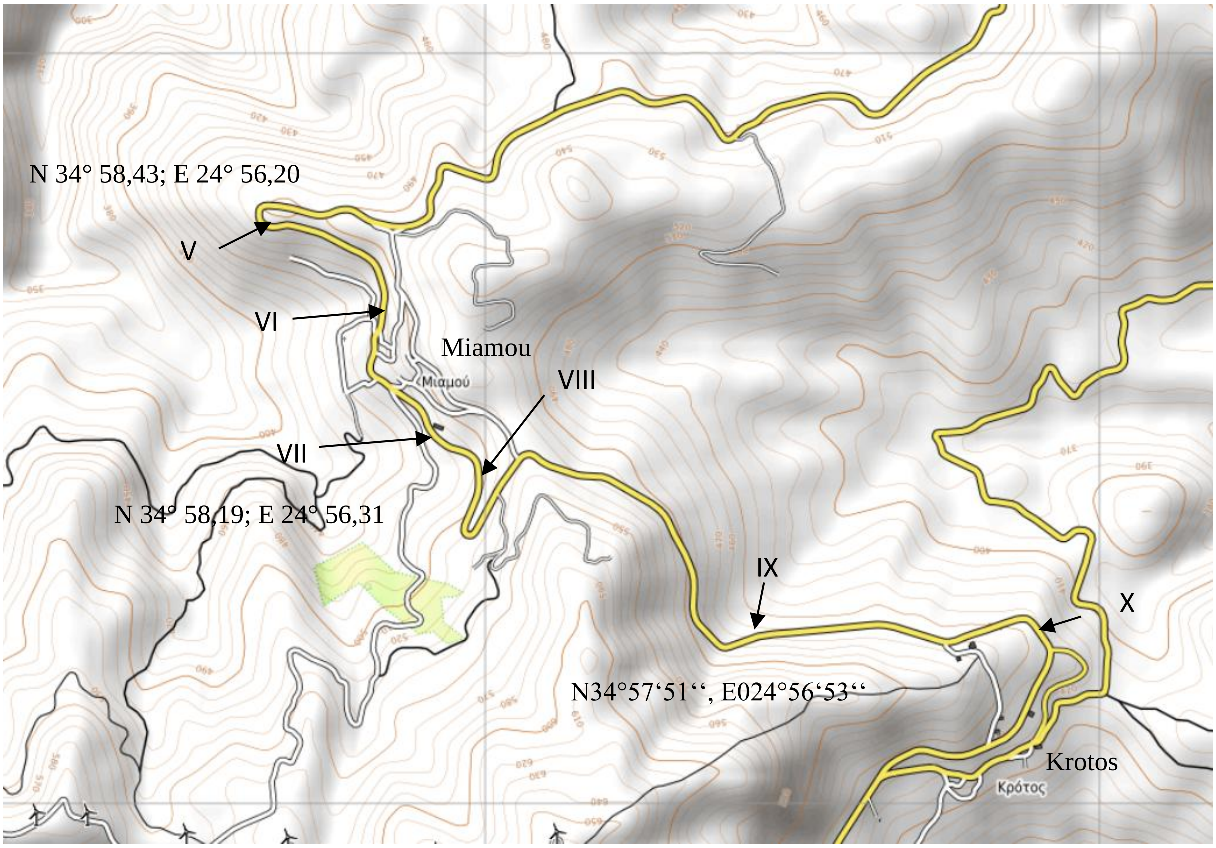

Location of outcrops

Outcrop V (N 34° 58.43; E 24° 56.20), Miamou Nappe, normal faults in 1: Flysch, 2: Mafic to andesitic volcanic rock (diabase).

Outcrop V, close up showing weathered and fresh rock surfaces. The light grey colour indicates the rock to be of andesite composition.

Outcrop VI, Miamou Nappe, basalt/andesite

Outcrop VI, Miamou Nappe, basalt/andesite

Outcrop VII (N 34° 58.19; E 24° 56.31), Miamou Nappe, limestone outcropping at the eastern side of Miamou village

Outcrop VII, closeup of previous picture. The limestone is reported to contain fossil coral fragments and is thought to be of Upper Jurassic age.

Outcrop VIII, Miamou Nappe, red and grey silty phyllite are reported to contain Upper Jurassic fossils and to correlate with the "Vatos Schists" south of the Kredos Mountain approx. 40km further northwest. The surrounding sandy-clayey layers of the Miamou Nappe are of very low grade metamorphism.

On the way to Krotos, one passes a part of the nappe that consist of serpentinized ultramafic rock. As a whole the nappe in the surrounding area is describes as being about 2 km thick, with the ultramafic rocks reaching a thickness of 250m. The rock is highly tectonically deformed and metamorphically overprinted *[Kull U., 2012]*.

Outcrop IX, Miamou nappe: mafic to ultramafic rocks embedded in phyllite-schist / mélange.

Outcrop IX, The green coloring could indicate the formation of chlorite and low-grade green schist metamorphism. The chlorites are a group of phyllosilicate minerals common in low-grade metamorphic rocks and in altered igneous rocks.

Outcrop IX, contact to country rock consisting of phyllite (flysch)

Outcrop IX, contact to country rock displaying highly sheared texture

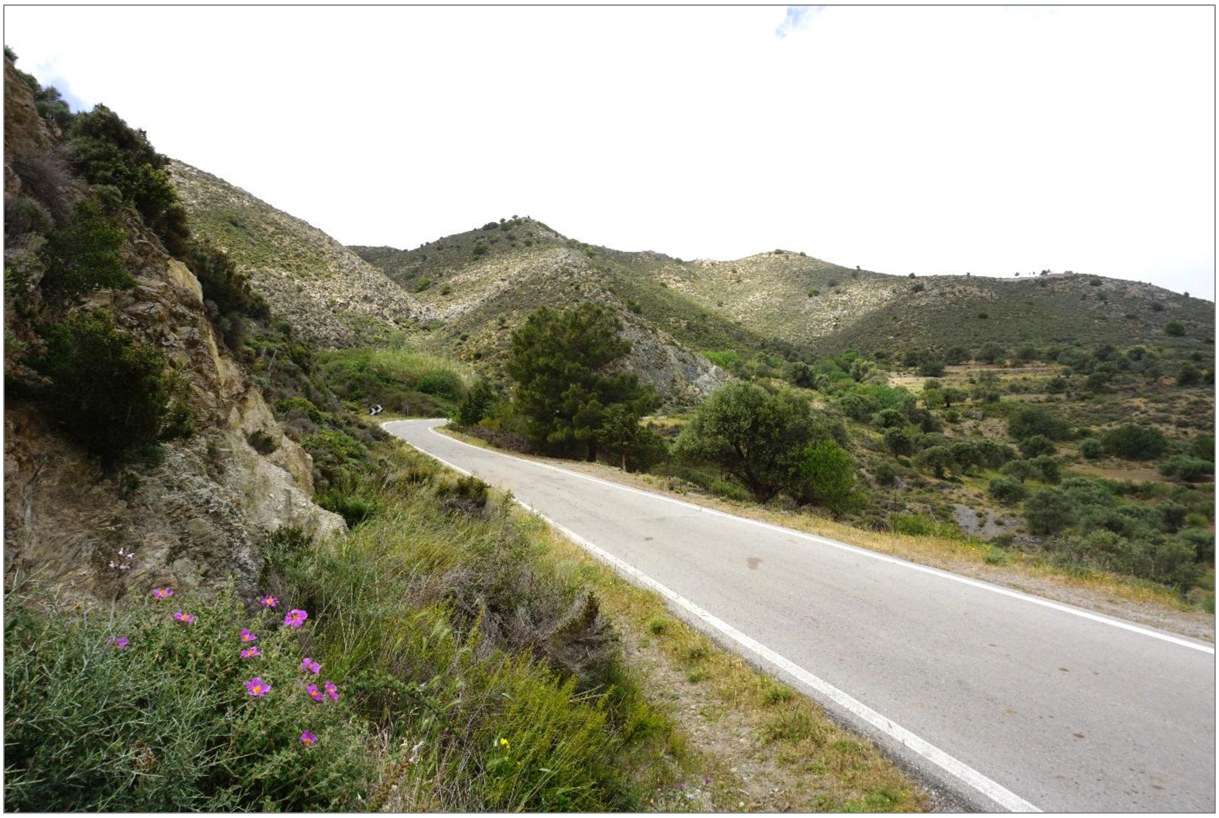

Outcrop IX: View of the Miamou Nappe landscape looking westwards. The mountain ridges consist of Jurassic fossiliferous limestone. Ophiolite mélange occasionally crops out along the road and on the mountain slopes.

Outcrop X: Miamou Nappe, ophiolitic mélange

Outcrop X. Miamou Nappe. At this location the ophiolitic mélange appears to be of sedimentary nature as there is no sign of shear surfaces such a rotation of clasts.

Large-scale mélanges formed in active continental margin settings generally consist of altered oceanic crustal material and blocks of continental slope sediments in a sheared mudstone matrix. The mixing mechanisms in such settings may include tectonic shearing forces, ductile flow of a water-charged or deformable matrix (such as serpentinite), sedimentary action (such as slumping, gravity-flow, and olistostromal action), or some combination of these. Some larger blocks of rock may be as much as one kilometre across. *[Wikipedia]*

Outcrop X. Miamou Nappe, ophiolitic mélange consisting of a chaotic mixture of sedimentary and mafic to ultramafic rocks

The village of Krotos lies mainly on Jurassic sandstones and marls of the Miamou nappe. Following the road westwards from Krotos one reaches the metamorphic rocks of the Asterousia Crystalline Complex (ACC) *[Kull U., 2012]*.

4 Asterousia Crystalline Complex

The Asterousia Crystalline Complex (ACC) consists largely of high-grade metasediments rocks and occasional metagranitoids veins and sills (Langosch et al. 2000; Martha et al. 2019). In contrast to the other uppermost subnappes the ACC can be correlated with the southern margin of the Pelagonian domain. It can therefore be associated with the Internal Hellinides (e.g. Aubouin & Dercourt, 1965; Bonneau, 1972; Martha et al. 2017). The ACC rocks consisting of amphibolites, quartzites, gneisses, and schists have undergone high-temperature/low-pressure metamorphism (P = 400–500 MPa, Tmax = 700 °C, Seidel et al. 1981). Characteristic metamorphic minerals are sillimanite, andalousite, cordierite, hornblende, garnet and biotite, which denote an upper amphibolite facies. Existing slices of serpentinite are thought to have been incorporated into the metasedimentary rocks prior to amphibolite facies metamorphism (Bonneau 1973; Reinecke et al. 1982; Be'eri-Shlevin et al. 2009) *[Zulauf et al, 2023]*.

The ACC-type rocks have been affected by polyphase deformation and metamorphism. Relics of an early phase of deformation are preserved as internal foliation in garnet porphyroblasts. A later phase of top-to-the SE shearing under upper amphibolite facies conditions took place during the Late Cretaceous and led to the dominant foliation, which can be observed today in the existing outcrops (Martha S. et al. 2017/2018). Rb-Sr radiometric dating confirms the existence of a Late Cretaceous thermal event as the ACC-type rocks - homogeneous paragneiss, migmatitic paragneiss and the granitoid rocks all have consistent biotite-whole-rock ages of about 72 Ma (Langosch A. et al. , 2000).

Regarding the origin of granitoid rocks in the ACC different models have been developed based on geochemical analysis. Langosch et al., 2000 indicates primary melts from migmatite paragneisses combined with fractional differentiation and assimilation of country rock to be a possible source of the granitoids and suggests the presents of a lower magma chamber providing the necessary heat for anatexis. However, he also states that there was probably some contribution of melts from lower-crust sources. Other authors propose that the granitoids are I-type granites with an arc (or fore-arc) related origin, which can be attributed to a subduction zone within the Pindos realm (Stampfli).

During the Middle Paleocene, the ACC was thrust on top of the other the nappes of the Uppermost Unit. The thrusting of the ACC-type rocks on top of the prehnite-pumpellyite facies Arvi Unit was initially under brittle conditions and remained to be in a top-to-the SE direction, which is the dominant kinematics of the Uppermost Unit on Crete. *[Martha S.]*

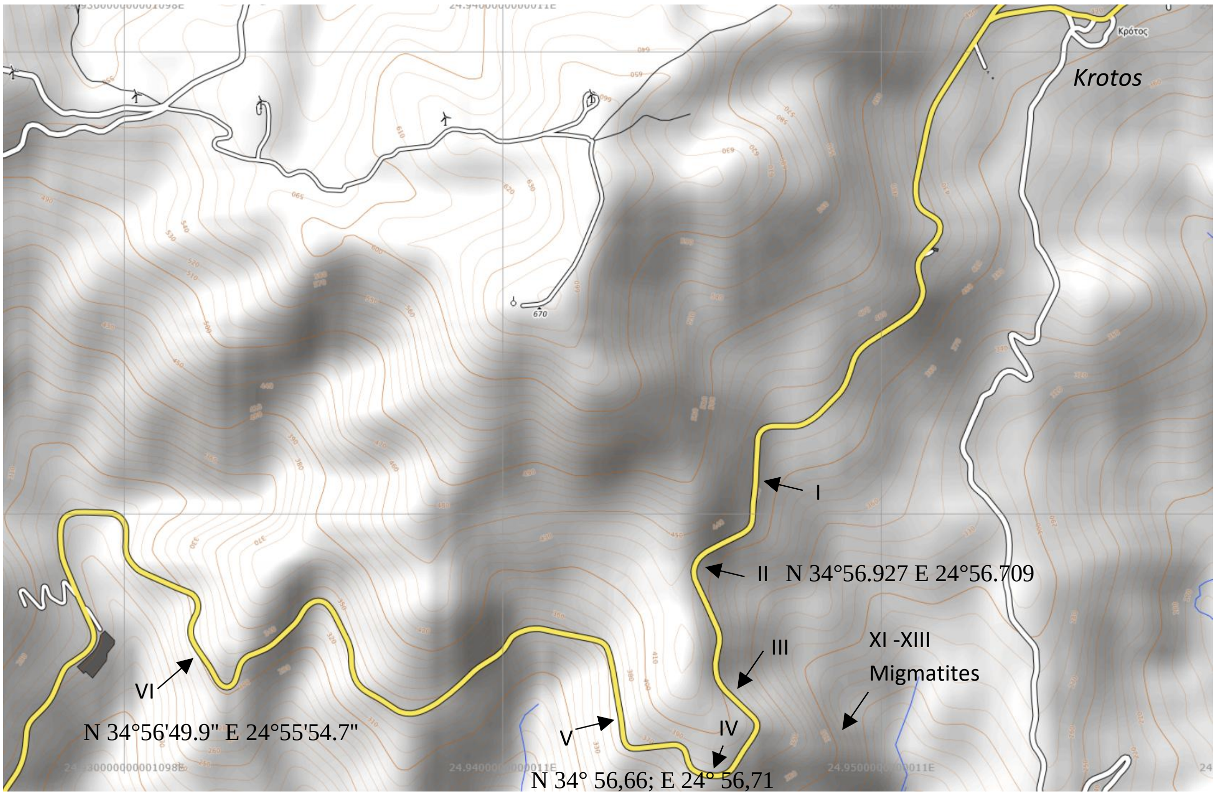

Location of Outcrops

Location of Outcrops [Image source: Google Maps]

4.1 Serpentinized Ultramafic Body

Along the main road just south of Krotos the first metamorphic rocks to be observed are light-colored mica schists *[Kull]*. The high-temperature/low-pressure (HT/LP) metamorphic rocks frequently alternate with outcrops of basaltic rock, which are sometimes in the form of slope scree. Further down the road from Krotos approx. 1.4 km there is a small body of serpentinized ultramafic rock. The country rock comprising a number of lenses of metamorphic schist is highly sheared. In the contact zone of the intrusion there is some indication of either contact metamorphism or additional hydrothermal alteration (see outcrop I).

Outcrop I: Country rock and fault zone next to the serpentinite body. 1: undisturbed calc-silicate schist *(right of dashed line) 2: faut zone (left of dashed line) consisting of highly sheared lenses of predominantly metasedimentary rock. 3: Part of rucksack as scale.*

Outcrop I: Overview, 1: country rock, 2: fault zone, 4: serpentinized ultramafic body. 3: Rucksack for scale.

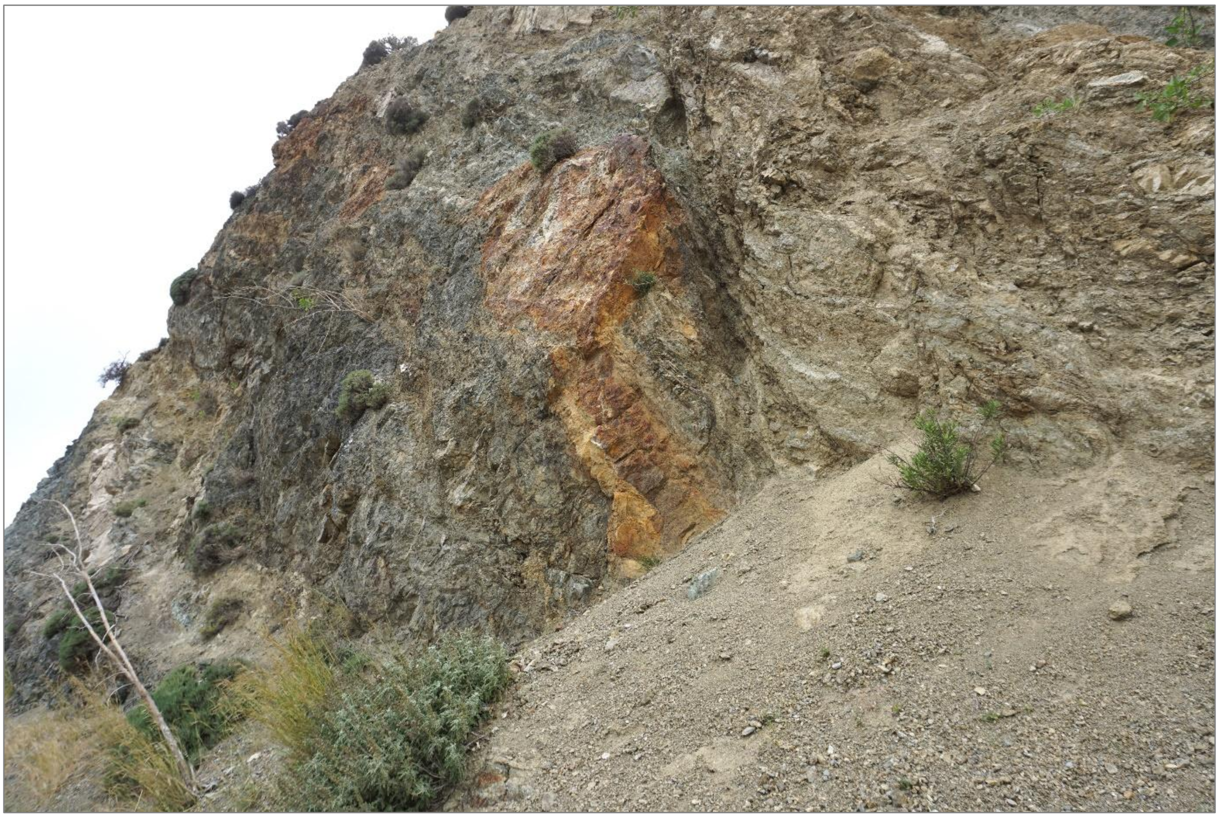

Outcrop I: faut zone, 2a: sheared calc-silicate schist, 2b: presumed hydrothermal vein, 2c: "mafic/ultramafic" highly sheared and partly cataclastic rock. 2d: marble lens

Outcrop I, 2b: hydrothermal vein displaying metal deposits (iron ?). Orange gangue rock could be former mafic /ultramafic rock.

Outcrop I, 2b: grab sample from the hydrothermal vein containing metal deposits (iron ?).

Outcrop I, 2b: Closeup of the hydrothermal vein. The gangue rock could be former mafic /ultramafic rock.

Outcrop I, 2c: highly sheared and partly cataclastic rock probably of mafic/ultramafic composition.

Outcrop I, closeup of previous picture, 2c: cataclastic rock probably of mafic/ultramafic composition (arrow)

Outcrop I, 2c: cataclastic mafic/ultramafic rock. 2d: overview of the marble lens and its shear zones, 3: rucksack for scale, 4: serpentinized ultramafic rock

Outcrop I, 4: Serpentinized ultramafic rock, 3: rucksack for scale

Outcrop I, closeup of previous picture. Serpentinized ultramafic rock

Outcrop I: Serpentinized ultramafic rock

4.2 Origin of serpentinite bodies - Asterousia nappe vs Miamou nappe

Peridotites in the oceanic lithosphere are very high-temperature rocks and consequently the minerals they contain are unstable under normal crustal conditions. High-temperature minerals are especially unstable in the presence of water. So when uplifted to become part of the oceanic lithosphere, original olivine and pyroxenes typically are metamorphosed by seawater to produce a variety of different hydrous minerals. Further hydration also occurs during tectonism associated with subduction zones.

During continental collision and obduction, ophiolites may become incorporated into mountain belts to become bodies of rock referred to as alpine peridotites. These peridotite bodies range from small slivers to large plutons. Often the peridotites are dismembered pieces – all that remain of once more complete oceanic lithosphere. Alpine peridotites typically contain serpentinized rocks (see Appendix for details on ophiolite emplacement).

Serpentine is a two sheet silicate with the formula $Mg3[Si_2O_5](OH)^-{}_4$). Its crystal structure is trioctahedral with a Mg:Si ratio of 3:2; it is stable up to 600°C at 1 GPa. Beyond that it is becomes unstable and is transformed from antigorite to forsterite + talc + H_2O. Presuming that the serpentinite was incorporated in to the sediments of the Asterousia Mts prior to HT/LP metamorphism, which took place during the Upper Cretaceous, the serpentinite would have been changed back to a more stable state such as an olivine bearing ultramafic rock. As the ultramafic rock is today again serpentinized it must have under undergone retrograde metamorphism. Alternatively, the serpentine could belong to the Miamou Nappe which was not exposed to high grade metamorphism *[Wasmann S.]*.

Outcrop II. Another ultramafic body approx. 200m further South. Rucksack for scale.

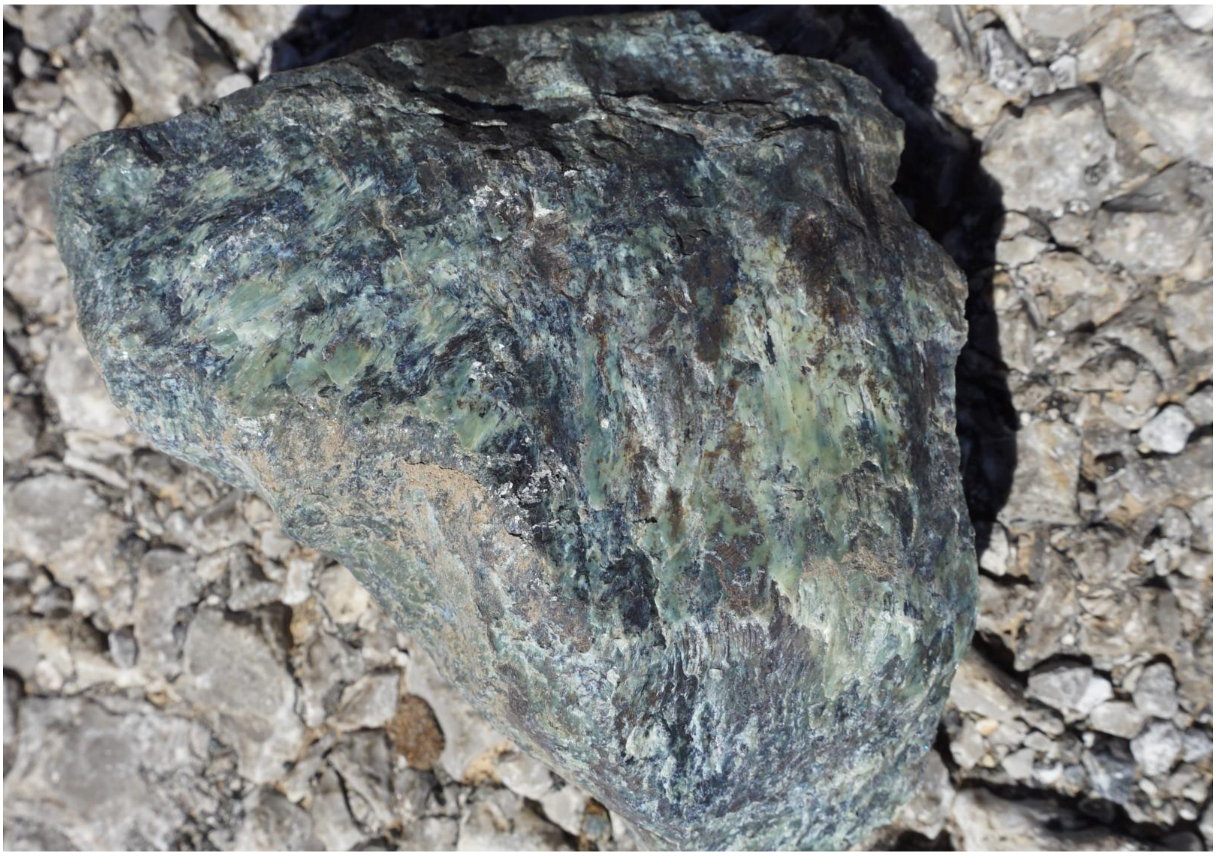

Outcrop II, Serpentinite grab sample

Outcrop II, fresh surface of ultrabasic rock sample

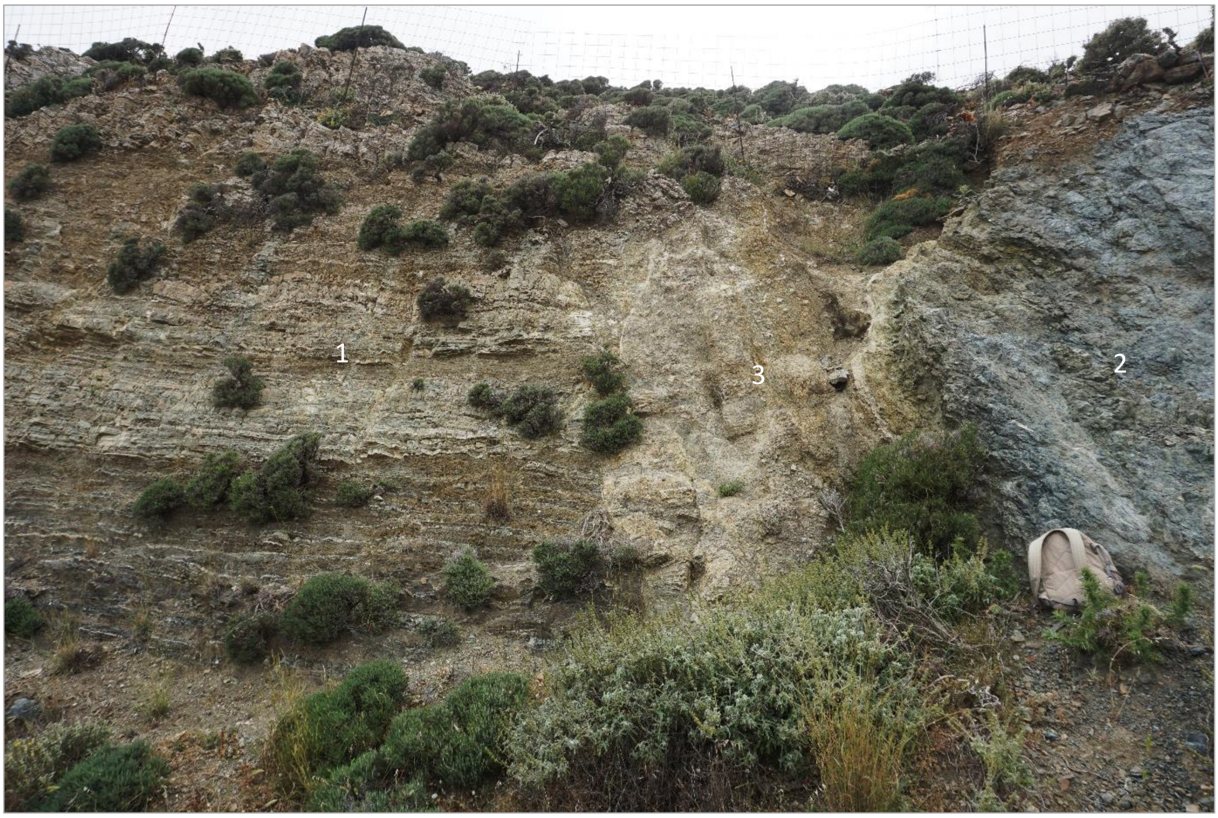

Outcrop II, Contact to the country rock. 1: Calc-silicate rock, 2: Ultramafic rock (serpentinite), 3: fault zone

4.3 Calc-Silicate Schist

The road descending to Lentas provides a section of gneisses that make up the Asterousia nappe (see following image by Koepke & Seidel, 1984). The section is over 1000 m thick, probably due to normal faulting and shear tectonics causing a repeat of parts of the sequence. The layers dip moderately (25°- 40°) towards the North. The dominant gneisses consisting of garnet mica schists are metamorphic pelites (i.e. former fine grained sedimentary rock such as i.e. mudstone or siltstone). The upper part of the section also displays, calc-silicate schists with occasional marble lenses.

The lower part of the section is reported to contain ortho-amphibolite (i.e. protolith of magmatic origin) (Koepke & Seidel, 1984). Pronounced schistosity is apparent in some places and folding is reported to be syn-metamorphic *[Kull]*.

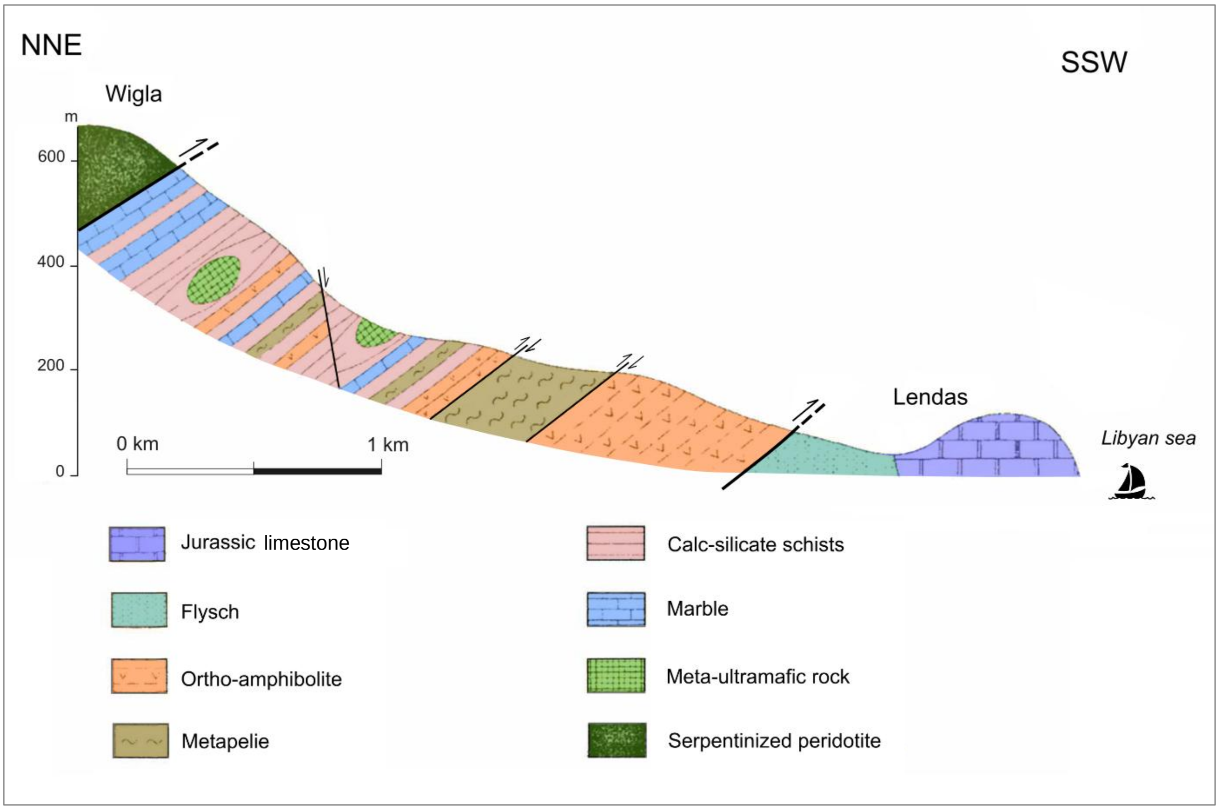

Section showing the rock exposed between Krotos and Lentas (Koepke & Seidel, 1984) [Kull]

Outcrop III. HT/LP metamorphic calc-silicate rock. 1: predominantly calcareous layers, 2: predominantly silicate containing layers. Rectangle: see next picture. Despite HT-LP-Metamorphism (P = 0,3 – 0,4 GPa, T = 600 – 750°C) the sedimentary bedding is still preserved.

Outcrop III. Migmatite: 1: Signs of anatexis (i.e. melting)

Outcrop III, Sample from the predominantly silicate containing layer. 1: leucosome

Outcrop III, Sample from a marble layer within the calci-silicate rock

Location of outcrops

Outcrop IV (N 34° 56.66; E 24° 56.71). *View of the Lentas peninsular looking south-eastwards*

The hill or peninsular at Lentas that is attributed to the Lentas unit is interpreted by some to be a tectonic mélange (Bonneau 1972 a, b, Bonneau et al. 1977) and displays similarity with the Arvi unit. However, investigations by Vandelli et al. 2010, Stampfli revealed the presence of Permian rocks and Triassic pelagic limestones which places the Lentas unit at the base of the Pindos unit (see My GeoGuide No. 23: The Uppermost Nappes in the Asterousia Mountains, Coast Road Platia Permata to Lutra).

4.4 Greenschist?

Outcrop IV, Greenschist ? displaying foliation and probably epidot veins.

Based on macroscopic assessment the green foliated metamorphic rock outcropping at this location is presumably a greenschist.

Martha et al. 2017 have investigated an area approx. 38 km the NW of the ACC near Melambes with lithology similar to the Asterousia Mts. He describes calc-silicates, orthogneisses, diorites, pelagic limestone (marbles) and a greenschist unit that is less metamorphic than the surrounding rock and is therefore thought to have been overthrust by the higher grade rocks in the area. The greenschist unit, also called the "Akoumianos Greenschist" is a fine-grained epidote-amphibole schist and displays pervasive foliation. Geochemically, it has a mid-ocean ridge basalt (MORB) -type signature (Reinecke et al. 1982; Martha et al. 2017) *[Martha]*.

Outcrop IV, closeup of samples of the "greenschist" shown above

4.5 Marble Layer in Calc-Silicate Schist

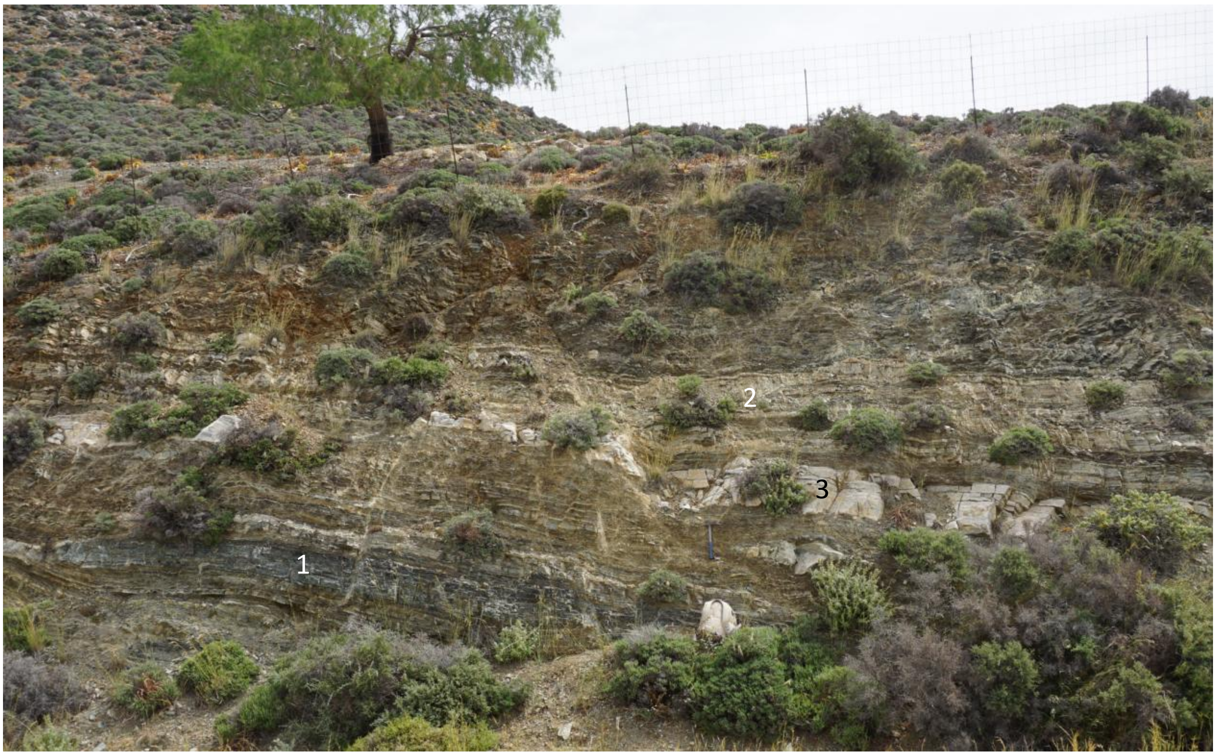

Outcrop V. calc-silicate schist 1: dark predominantly silicate containing layers, 2: light predominantly calcareous layers, 3: marble layer

Outcrop V. 1: The dark layers of the calc-silicate sequence.

Outcrop V. Closeup of previous picture

Outcrop V. Sample from the marble layer within the calc-silicate schist

4.6 Pegmatite Vein

Outcrop VI. 1: Granitoid vein, 2: calc-silicate schist, 3: rucksack for scale. Rectangles: enlargements see following pictures

Outcrop VI a. Granitoid vein in calc-silicate schist. The rock is pegmatitic (i.e. coarse grained) and was intruded into the existing calc-silicate schist.

Outcrop VI a. Closeup of previous picture displaying pegmatitic texture of the granitoid vein and the contact to the calc-silicate schist.

The granitoid magma is thought to be melt from of deeper lying migmatites (i.e. leucosome). At the time of intrusion, the country rock must have been quite hot otherwise the intruded magma would have cooled quickly at its edges and become fine grained. Another indication of high temperature of the country rock is that there is no sign of fritting at the contact to the magma. In addition, the country rock (calc-silicate schist) is slightly folded, which indicates high temperatures and ductile deformation. The foliation is parallel to bedding and some layers display boudinage *[Wasmann S.]*.

Outcrop VI b. Granitoid vein in calc-silicate schist.

4.7 Amphibolite

Outcrop VII Ortho-amphibolite

Outcrop VII: Ortho-amphibolite

Outcrop VII: Ortho-amphibolite

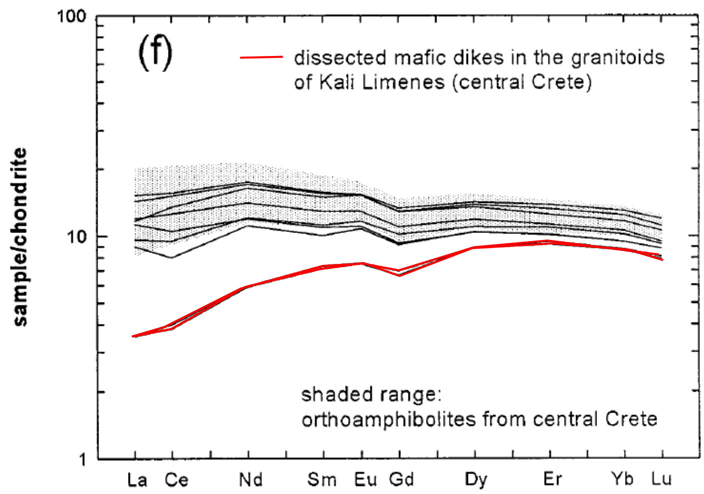	*REE patterns for ortho-amphibolites from the Lentas-Kali Limenes area and nonfoliated mafic dykes in the granitoids of Kali Limenes (central Crete) [Langosch A. et al. , 2000].*

It is worth noting that orthoamphibolites widespread in the metamorphic country rock sequence of the Asterousia Mountains are geochemically indistinguishable from the nonfoliated mafic dikes in the granitoids of Kali Limenes *[Langosch A. et al. , 2000]*. (See My GeoGuide No. 22: The Uppermost Nappes in the Asterousia Mountains - Coast Road Kali Limenes to Chrysostoms). In contrast the trace element contents (i.e. Zr, Nb, Y , Hf, Th, U, Zn) of the mafic dikes differ significantly from the diorites of the Asterousia Mts found near Lentas/Gerokampos.

4.8 Magmatic Vein and Carbonate Layer

Outcrop VIII. Metamorphic magmatic vein of andesitic or mafic composition in calc-silicate schist. 1: magmatic vein, 2: marble layer, 3: calc-silicate schist.

Outcrop VIII. Magmatic vein. The vein is reported to be metamorphic and of andesitic or mafic composition. It cuts across the layering of the calc-silicate rock (i.e. discordant) and is thought to have been intruded prior to metamorphism. During metamorphism the vein was folded and deformed along with the country rock [Wassmann S.].

Outcrop VIII. Closeup of magmatic vein displaying porphyroblastic texture. 1: small plagioclase Porphyroblasts (i.e. relatively large single crystals, which formed by metamorphic growth in a more fine-grained matrix).

Outcrop VIII. Marble layer within the calc-silicate schist displaying boudinage of layers.

Outcrop VIII. Sample of marble from the marble layer

4.9 Major Fault

Outcrop IX (N34°56‘09‘‘, E024°55‘12‘‘). Reverse fault at the tectonic contact presumably between flysch (left) and calc-silicate schist (right). Apatite fusion track ages indicate that the flysch was once heated (but not high enough to achieve metamorphism) and cooled quickly through the apatite partial annealing zone at about 14.0 Ma and 17.7 Ma. [Thomson S. N., 1998]. The calc-silicate schist is thrust upon the flysch rocks (see drawing by Koepke & Seidel, 1984) [Kull].

5 Migmatites south of Krotos

Location of Outcrops [Image source: Google Maps]

About 2.5 km from Krotos migmatite rocks crop out half way down the mountain slope about 200m below the main road. While undertaking an approx. 1.5 hour hike along the dirt road from Krotos one encounters “Pindos“ limestone and ultramafic slope talus.

5.1 Ophiolite Talus

Outcrop X: Slope talus consisting of a mixture of ultramafic rocks. Some of the boulders appear to be purly igneous (or alteratively high grade metamorthic) while, others seem to be serpentinized - a form of hydrous alteration at lower tempertures.

Outcrop X, close up of previous picture: sample displaying large pyroxene or amphibole crystals in a dark matrix. 1: pyroxene or amphibole crystal; 2: dark matrix; 3: braun mineral that could be iddingsite - weatheing product of olivine. The green boulder on the right is probably serpentinite.

5.2 Migmatites

Outcrop XI: View of the valley looking south towards the yacht harbour. 1:Migmatite rock rims the bottom of the picture, 2: Pindos limestone, 3: Basalt, red shales, sandstone [Vachard D., Stampfli, 2010]

Outcrop XI: Migmatite displaying schlieren structure due to partial melting. 1: Garnet

The principal parts of a migmatite are: a) the mesosome (or palaeosome), which represents the more or less unaltered, metamorphic parent rock, b) the leucosome, which is usually significantly lighter in colour compared to the mesosome, i.e. it contains more quartz and feldspar and shows no favoured orientation of its mineral grains, and c) the melanosome, which is enriched in dark (mafic) minerals, such as biotite or amphibole, and which usually occurs at the boundary between mesosome and leucosome. See also My GeoGuide “No. 22: The Uppermost Nappes in the Asterousia Mountains - Coast Road Kali Limenes to Chrysostoms” for further examples of migmatites.

Outcrop XI: Close up of previous picture. 1: mesosome, 2: leucosome (feldspar and quartz), 3: melanosome, which often forms a thin boundary next to the leucosome.

Outcrop XII: Migmatite with large leucosomes.

Outcrop XII: Close up of previous picture. 1: mesosome, 2: leucosome (feldspar and quartz), 3: garnet 4: tourmaline. Tourmaline is recognizable by its rounded triangular shape and its poor cleavage. Garnets are present in both the mesosome and the leucosome. This has some relevance as garnet of a similar composition may be found in the granitoid veins near Kali Limenes. According to Langosch A. et al., 2000 the magmatic garnet is most likely the result of chemical interaction with the country rock consisting of paragneiss (i.e same geneisses as the ones at this location.)

Outcrop XII: Migmatite displaying "schlieren structure"

Outcrop XII: Large "Augen" shaped feldspars within the mesosome reminisent of augengneiss. The mesosome of the migmatites is reported to contain the metamorphic minerals cordierite and sillimanite. HT/LP-Metamorphism and intrusion of granitoid magma (near Kali Limenes) took place simultaneously during the late Cretaceous (72 Ma) [Langosch A. et al. , 2000].

Outcrop XIII: Migmatite with schleren structure. 1: leucosome with tourmaline. 2: garnet, garnets are present both within the leucosome and mesosome.

Outcrop XIII: Migmatite with schleren structure and leucosome veins

Langosch A. et al. (2000) suggests that intrusion of mafic melts at depth acted as a heat source, elevating mid-crustal regions to amphibolite-facies temperatures and causing the formation of migmatitic paragneisses.

5.3 Hypotheses

Regarding the gneisses and migmatite rocks particularly deep within the in the valley leading to Krotos, no marble or calcsilicate rocks were encountered. Former existing calcsilicate rocks might have released CO_2 and CaO thereby influencing the fluid-solidus curve and lowering the melting point for the leucosome within the migmatites.

Under the same pressure and temperature conditions, it is more likely that a calc-silicate rock will form a migmatite than a pure silicate rock. Calc-silicate rocks containing $CaCO_3$ can release CO_2 under metamorphic conditions. This lowers the melting point and facilitates partial melting. CO_2 along with H_2O therefore play a crucial role in melting. Carbonate phases react with melts and minerals, increasing the mobility of the melt and promoting the formation of migmatites.

6 References

Alexandra van der Geer1 & George Lyras, 2011: Field Trip Guidebook European Association of Vertebrate Palaeontologists, 9th Annual Meeting Heraklion, Crete, Greece 14-19 June, 2011

Alves, T. Cupkovic T., 2018: Footwall degradation styles and associated sedimentary facies distribution in SE Crete: Insights into tilt-block extensional basins on continental margins; 3D Seismic Lab, School of Earth and Ocean Sciences, Cardiff University, Cardiff, United Kingdom; Husky Energy, Atlantic Region, 351 Water St., Suite 105, St. John's, Canada

Brandes C. et al., 2014: Fault-related folding: A review of kinematic models and their application, Institute for Geology, Leibniz Universität Hannover, Callinstr. 30, 30167 Hannover, Germany

Champod E. et al., 2010: Stampfli Field Course: Tectonostratigraphy and Plate Tectonics of Crete, Université de Lausanne, September 2010

Chatzaras, v., Xypolias, P. & Doutsos, T (2006): Exhumation of high-pressure rocks under continuous compression: a working hypothesis for the southern Hellenides (central Crete. Greece). - Geol. Mag. 143: 859-R76.

Cowan (1985), Gesteine bestimmen, Teil 2: Minerale
https://www.kristallin.de/gesteine/index.htm

Fassoulas C., 2000: The tectonic development of a Neogene basin at the leading edge of the active European margin: the Heraklion basin, Crete, Greece, Natural History Museum of Crete, University of Crete, Heraklion 71409, Greece

Fassoulas C., Rahl J.M., 2004: Patterns and Conditions of Deformation in the Plattenkalk Nappe, Crete, Greece: A Preliminary Study, Natural History Museum of Crete, Yale University, New Haven, Connecticut

Granger D.E., 2007: Cosmogenic Nuclide Dating - Landscape Evolution, in Encyclopedia of Quaternary Science, Pages 445-452

Kull U., 2012: Kreta, Sammlung geologischer Führer

Lacinska A. M. et. al., 2016: Mineralogical characterisation of serpentine minerals in the context of carbon capture and storage by mineralization. Preliminary results, British Geological Survey, Environmental Science Centre, Nicker Hill, Keyworth, Nottingham NG12 5GG, United Kingdom

Langosch A. et al, 2000: Intrusive rocks in the ophiolitic melange of Crete ± Witnesses to a Late Cretaceous thermal event of enigmatic geological position, Institut für Mineralogie und Geochemie, Universität zu Köln.

Martha S. et. al., 2018: The tectonometamorphic evolution of the Uppermost Unit south of the Dikti Mountains, Crete Institut für Geowissenschaften, Goethe-Universität Frankfurt

Martha S. et al., 2017: The tectonometamorphic and magmatic evolution of the Uppermost Unit in central Crete (Melambes area): constraints on a Late Cretaceous magmatic arc in the Internal Hellenides (Greece); Institut für Geowissenschaften, Goethe-Universität Frankfurt
*

McClay K.R.: Glossary of thrust tectonics terms, Department of Geology, Royal Holloway and Bedford New College, University of London, Egham, Surrey, England

Miller W., 1977: Geologie des Gebites Nördlich des Plakias-Bucht, Kreta, Freiburg im Breisgau, Diplomarbeit

Mountrakis D., Kilias A., Pavlaki A., Fassoulas C., Thomaidou E., Papazachos C., Papaioannou C., Roumelioti Z., et al., 2012: Neotectonic study of Western Crete and implications for seismic hazard assessment, Journal of the Virtual Explorer, Electronic Edition, ISSN 1441-8142, volume 42, paper 2 In: (Eds.) Emmanuel Skourtsos and Gordon S. Lister, The Geology of Greece, 2012.

Ogata K. et. al., 2013: Mélanges in flysch-type formations: Reviewing geological constraints for a better understanding of complex formations with block-in-matrix fabric, Universita` degli Studi di Napoli Federico II, Dipartimento di Scienze della Terra

Palamakumbura R. et. al., 2012: Geochemical, sedimentary and micropaleontological evidence for a Late Maastrichtian oceanic seamount within the Pindos ocean (Arvi Unit, S Crete, Greece), School of GeoSciences, University of Edinburgh, West Mains Road, Edinburgh, EH9 3JW, UK

Pirazzoli P.A., Thommeret J., Thommeret Y., Laborel J., and Montaggioni L.F., 1982: Tectonophysics 86, 27-43.

Pomoni F., Karakitsios V., 2016: Sedimentary facies analysis of a high-frequency, small-scale, peritidal carbonate sequence in the Lower Jurassic of the Tripolis carbonate unit (central western Crete, Greece): Long-lasting emergence and fossil laminar dolocretes horizons, Department of Geology and Geoenvironment, National and Kapodistrian University of Athens

Rahl J. M. et. al.: Exhumation of high-pressure metamorphic rocks within an active convergent margin, Crete, Greece: A field guide, Jeffrey M. Rahl, Charalampos, Fassoulas, and Mark T. Brandon, Department of Geology and Geophysics, Yale University, New Haven, Connecticut 06511, U.S.A. Natural History Museum of Crete, University of Crete, Heraklion 71409, Greece

Rieger S., 2015: Regional-Scale, Natural Persistent Scatterer Interferometry, Island of Crete (Greece), and Comparison to Vertical Surface Deformation on the Millennial-, and Million-Year Time-Scales; Phd.; Ludwig-Maximilians-Universität München

Seidel M., 2003: Tectono-sedimentary evolution of middle Miocene supra-detachment basins (western Crete, Greece), Ph.D. Dissertation, University of Köln.

Stampfli 2010: Stampfli Field Course, Tectonostratigraphy and Plate Tectonics of Crete, Université de Lausanne, France

Steiakakis E., 2017: Evaluation of Exploitable Groundwater Reserves in Karst Terrain: A Case Study from Crete; Greece Laboratory of Applied Geology, Technical University of Crete, 73100 Chania, Greece

Thomson S. N. et al., 1998: Apatite fission-track thermochronology of the uppermost tectonic unit of Crete, Implications for the post-Eocene tectonic evolution of the Hellenic Subduction System, Institut für Geologie, Ruhr-Universität Bochum

Thomson S. N., Stockert B., Brix M. R., 1999. Miocene high-pressure metamorphic rocks of Crete, Greece: rapid exhumation by buoyant escape. In: Ring, U., Brandon M. T., Lister G. S., Willetf S. D. (eds): Exhumation Processes: Normal Faulting, Ductile Flow and Erosion. Geological Society, London, Special Publications, 154, 87-107.

Thomson S. N., Stockhert, B. & Brix, M.R. (1998a): Thennochronology of the high-pressure metamorphic rocks of Crete, Greece: implications for the speed of tectonic processes. - Geology 26: 259-262.

Thrust faults: Some common terminology - Geological Digressions https://www.geological-digressions.com

Tiberti M. M., Basili R. & Vannoli P., 2014: Ups and downs in western Crete (Hellenic subduction zone), Istituto Nazionale di Geofisica e Vulcanologia, Via di Vigna Murata 605, 00143 Rome, Italy

Theye, T, Seidel, E. & Vidal, O. (1992): Carpholite, sudoite and chloritoid in low-grade high-pressure metapelites from Crete and the Peloponnese, Greece. - Europ, J. Mineral.4 487-507.

Tortorici L., 2011: The Cretan ophiolite-bearing mélange (Greece): A remnant of Alpine accretionary wedge, Dipartimento di Scienze Geologiche, University of Catania, C.so Italia 55, 95129 Catania, Italy

van Hinsbergen D. J. J., Meulenkamp J. E., 2006: Neogene supradetachment basin development on Crete (Greece) during exhumation of the South Aegean core complex.

Vassilakis E. and Alexopoulos J., 2012: Recognition of Strike-slip Faulting on the Supradetachment Basin of Messara (Central Crete) with remote sensensing Image Interpretation Techniques; National and Kapodistrian University, Department of Dynamics, Tectonics and Applied Geology, Athens, Greece; National and Kapodistrian University, Department of Geophysics & Geothermics, Athens, Greece;

Wassmann S., 2012 Geländekurs Kreta

Zachariasse W., van Hinsbergen D., et al. 2011, Formation and Fragmentation of a late Miocene supradetachment basin in central Crete: implications for exhumation mechanisms of high-pressure rocks in the Aegean forearc, Stratigraphy and Paleontology group, Faculty of Geosciences, Utrecht University, Utrecht, The Netherlands; Physics of Geological Processes, University of Oslo

7 Appendix

Geological Time Scale

Eonothem/ Eon	Erathem/ Era	System/ Period	Series/ Epoch	Stage/ Age	mya[1]
Phanerozoic	Cenozoic	Neogene	Pliocene		2.58
Phanerozoic	Cenozoic	Neogene	Pliocene	Piacenzian	3.600
Phanerozoic	Cenozoic	Neogene	Pliocene	Zanclean	5.333
Phanerozoic	Cenozoic	Neogene	Miocene	Messinian	7.246
Phanerozoic	Cenozoic	Neogene	Miocene	Tortonian	11.63
Phanerozoic	Cenozoic	Neogene	Miocene	Serravallian	13.82
Phanerozoic	Cenozoic	Neogene	Miocene	Langhian	15.97
Phanerozoic	Cenozoic	Neogene	Miocene	Burdigalian	20.44
Phanerozoic	Cenozoic	Neogene	Miocene	Aquitanian	23.03
Phanerozoic	Cenozoic	Paleogene	Oligocene	Chattian	27.82
Phanerozoic	Cenozoic	Paleogene	Oligocene	Rupelian	33.9
Phanerozoic	Cenozoic	Paleogene	Eocene	Priabonian	37.8
Phanerozoic	Cenozoic	Paleogene	Eocene	Bartonian	41.2
Phanerozoic	Cenozoic	Paleogene	Eocene	Lutetian	47.8
Phanerozoic	Cenozoic	Paleogene	Eocene	Ypresian	56.0
Phanerozoic	Cenozoic	Paleogene	Paleocene	Thanetian	59.2
Phanerozoic	Cenozoic	Paleogene	Paleocene	Selandian	61.6
Phanerozoic	Cenozoic	Paleogene	Paleocene	Danian	66.0
Phanerozoic	Mesozoic	Cretaceous	Upper	Maastrichtian	72.1 ± 0.2
Phanerozoic	Mesozoic	Cretaceous	Upper	Campanian	83.6 ± 0.2
Phanerozoic	Mesozoic	Cretaceous	Upper	Santonian	86.3 ± 0.5
Phanerozoic	Mesozoic	Cretaceous	Upper	Coniacian	89.8 ± 0.3
Phanerozoic	Mesozoic	Cretaceous	Upper	Turonian	93.9
Phanerozoic	Mesozoic	Cretaceous	Upper	Cenomanian	100.5
Phanerozoic	Mesozoic	Cretaceous	Lower	Albian	~113
Phanerozoic	Mesozoic	Cretaceous	Lower	Aptian	~125.0
Phanerozoic	Mesozoic	Cretaceous	Lower	Barremian	~129.4
Phanerozoic	Mesozoic	Cretaceous	Lower	Hauterivian	~132.9
Phanerozoic	Mesozoic	Cretaceous	Lower	Valanginian	~139.8
Phanerozoic	Mesozoic	Cretaceous	Lower	Berriasian	~145.0

Eonothem/ Eon	Erathem/ Era	System/ Period	Series/ Epoch	Stage/ Age	mya[1]
Phanerozoic	Mesozoic	Jurassic	Upper		~145.0
Phanerozoic	Mesozoic	Jurassic	Upper	Tithonian	152.1 ± 0.9
Phanerozoic	Mesozoic	Jurassic	Upper	Kimmeridgian	157.3 ± 1.0
Phanerozoic	Mesozoic	Jurassic	Upper	Oxfordian	163.5 ± 1.0
Phanerozoic	Mesozoic	Jurassic	Middle	Callovian	166.1 ± 1.2
Phanerozoic	Mesozoic	Jurassic	Middle	Bathonian	168.3 ± 1.3
Phanerozoic	Mesozoic	Jurassic	Middle	Bajocian	170.3 ± 1.4
Phanerozoic	Mesozoic	Jurassic	Middle	Aalenian	174.1 ± 1.0
Phanerozoic	Mesozoic	Jurassic	Lower	Toarcian	182.7 ± 0.7
Phanerozoic	Mesozoic	Jurassic	Lower	Pliensbachian	190.8 ± 1.0
Phanerozoic	Mesozoic	Jurassic	Lower	Sinemurian	199.3 ± 0.3
Phanerozoic	Mesozoic	Jurassic	Lower	Hettangian	201.3 ± 0.2
Phanerozoic	Mesozoic	Triassic	Upper	Rhaetian	~208.5
Phanerozoic	Mesozoic	Triassic	Upper	Norian	~227.0
Phanerozoic	Mesozoic	Triassic	Upper	Carnian	~237.0
Phanerozoic	Mesozoic	Triassic	Middle	Ladinian	~242.0
Phanerozoic	Mesozoic	Triassic	Middle	Anisian	247.2
Phanerozoic	Mesozoic	Triassic	Lower	Olenekian	251.2
Phanerozoic	Mesozoic	Triassic	Lower	Induan	251.902 ± 0.024
Phanerozoic	Paleozoic	Permian	Lopingian	Changhsingian	254.14 ± 0.7
Phanerozoic	Paleozoic	Permian	Lopingian	Wuchiapingian	259.1 ± 0.5
Phanerozoic	Paleozoic	Permian	Guadalupian	Capitanian	265.1 ± 0.4
Phanerozoic	Paleozoic	Permian	Guadalupian	Wordian	268.8 ± 0.5
Phanerozoic	Paleozoic	Permian	Guadalupian	Roadian	272.95 ± 0.11
Phanerozoic	Paleozoic	Permian	Cisuralian	Kungurian	283.5 ± 0.6
Phanerozoic	Paleozoic	Permian	Cisuralian	Artinskian	290.1 ± 0.26
Phanerozoic	Paleozoic	Permian	Cisuralian	Sakmarian	295.0 ± 0.18
Phanerozoic	Paleozoic	Permian	Cisuralian	Asselian	298.9 ± 0.15
Phanerozoic	Paleozoic	Carboniferous	Pennsylvanian[2] Upper	Gzhelian	303.7 ± 0.1
Phanerozoic	Paleozoic	Carboniferous	Pennsylvanian[2] Upper	Kasimovian	307.0 ± 0.1
Phanerozoic	Paleozoic	Carboniferous	Pennsylvanian[2] Middle	Moscovian	315.2 ± 0.2
Phanerozoic	Paleozoic	Carboniferous	Pennsylvanian[2] Lower	Bashkirian	323.2 ± 0.4
Phanerozoic	Paleozoic	Carboniferous	Mississippian[2] Upper	Serpukhovian	330.9 ± 0.2
Phanerozoic	Paleozoic	Carboniferous	Mississippian[2] Middle	Visean	346.7 ± 0.4
Phanerozoic	Paleozoic	Carboniferous	Mississippian[2] Lower	Tournaisian	358.9 ± 0.4

Open Petrology
Free Textbook for College-Level Petrology Courses

Ophiolites and Serpentinites

https://opengeology.org/petrology/13-metamorphism-of-mafic-rocks/#1371

Earth's mantle is made of ultramafic rocks. Peridotites, including mostly lherzolite, harzburgite, and dunite, dominate. At mid-ocean ridges, these ultramafic rocks rise to fill space created when plates diverge. This leads to decompression melting, creating mafic magmas that crystallize in the upper part of the lithosphere as gabbros, or that erupt as seafloor basalts.

Overall, the oceanic lithosphere consists of a thin part of the uppermost mantle (ultramafic), overlain by mafic and ultramafic crust, in turn overlain by thin layers of seafloor sediments. The lithosphere cools and becomes denser during seafloor spreading, and so sinks. Thus, the youngest seafloor and highest elevations are at the ridges, and the oldest seafloor and lowest elevations at ocean margins. The oceanic lithosphere may not be the same composition and structure everywhere, but all evidence suggests that there are some standard components. The evidence comes from many sources including drill core, seismic studies, laboratory experiments, grab sampling from the ocean floor, and dredging. The best information, however, may come from studies of ophiolites. The term ophiolite derives from the Greek words ophio (snake) and lite (stone), referring to the commonly green color of the rocks that make up ophiolites.

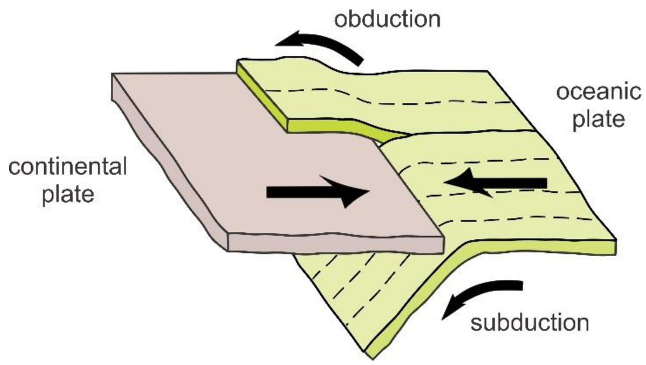

Obduction and subduction occurring at a subduction zone

Where oceanic and continental plates converge, oceanic lithosphere generally subducts beneath the continent. Sometimes, however, pieces of oceanic lithosphere are scraped off and added to a continent. We call this process obduction. Because of obduction, ultramafic rocks, formerly pieces of the mantle, can be found in ophiolite complexes. These complexes are wedges of ocean crust and mantle, now exposed in outcrops at the surface, that were thrust onto continental margins above subduction zones. Ophiolites are very important to geologists because they provide direct evidence for the nature of Earth's oceanic crust and upper mantle. Although there are many ophiolites around the world, most are small or very fragmented. Most ophiolites are 10s or 100s of millions of years old because the processes of sea-floor spreading and obduction are slow. The Macquarie Island Ophiolite, the youngest known, is still more than 10 million years old.

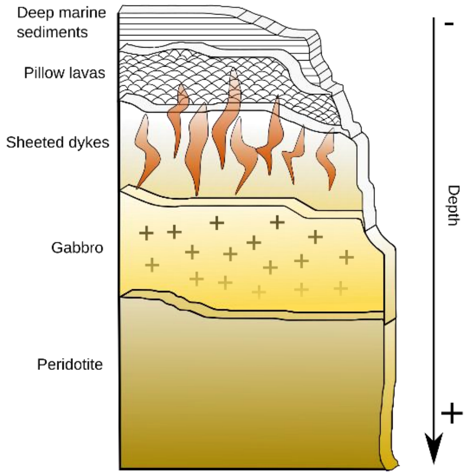

Stratigraphic sequence of an ophiolite (source: Wikipedia [Ophiolite - Wikipedia])

Every ophiolite provides a partial cross section of the oceanic lithosphere. When geologists combined information from many ophiolites with other evidence, a standardized model of the oceanic lithosphere. A "complete" ophiolite would include all the layers of rock shown in the figure above. These layers, which correspond to sediments and igneous rocks created by seafloor spreading, make up a cross section of the oceanic lithosphere. At its top, muds and other debris typically overlie hard rock. These sediments, which increase in thickness from mid-ocean ridges to ocean margins, may eventually lithify to form shale or chert. A layer of basalt, often containing pillow lavas, worm-like bodies formed during submarine eruptions, underlies the sediments. These basalts, like many ocean floor basalts, are commonly highly altered by interaction with seawater.

Magmas that create ocean-floor basalts rise from magma chambers below, following fractures and creating vertical, parallel, mafic dikes. The many dikes produce a sheeted dike complex beneath the basalts. At still greater depth, a thick layer of gabbro is the remains of once liquid basaltic magma chambers. The gabbro layer, accounting for most of the oceanic crust by volume, typically contains mafic to ultramafic cumulates in its lowest levels. The figure below6 is a photo of gabbro layers in the Troodos ophiolite – the browner layers contain significant amounts of orthopyroxene compared with the lighter colored layers. Peridotites (mainly harzburgites and lherzolites) of the oceanic mantle can be found beneath the gabbro layer.

Layered gabbro from the Troodos Ophiolite in Cyprus

The peridotites in the oceanic lithosphere are very high-temperature rocks and consequently the minerals they contain are unstable under normal crustal conditions. High-temperature minerals are especially unstable in the presence of water. So when uplifted to become part of the oceanic lithosphere, original olivine and pyroxenes typically are metamorphosed by seawater to produce a variety of different hydrous minerals. Further hydration also occurs during tectonism associated with subduction zones.

During continental collision and obduction, ophiolites may become incorporated into mountain belts to become bodies of rock we call alpine peridotites. These peridotite bodies range from small slivers to large plutons. Often the peridotites are dismembered pieces – all that remain of once more complete oceanic lithosphere. Alpine peridotites typically contain serpentinized rocks (see Appendix).

Ophiolite emplacement

[Ophiolite - Wikipedia]

There is yet no consensus on the mechanics of emplacement, the process by which oceanic crust is uplifted onto continental margins despite the relatively low density of the latter. All emplacement procedures share the same steps nonetheless: subduction initiation, thrusting of the ophiolite over a continental margin or an overriding plate at a subduction zone, and contact with air.

Scientists have drilled only about 1.5 km into the 6- to 7-kilometer-thick oceanic crust, so scientific understanding of oceanic crust comes largely from comparing ophiolite structure to seismic soundings of in situ oceanic crust. Oceanic crust generally has a layered velocity structure that implies a layered rock series similar to that listed above. But in detail there are problems, with many ophiolites exhibiting thinner accumulations of igneous rock than are inferred for oceanic crust. Another problem relating to oceanic crust and ophiolites is that the thick gabbro layer of ophiolites calls for large magma chambers beneath mid-ocean ridges. However, seismic sounding of mid-ocean ridges has revealed only a few magma chambers beneath ridges, and these are quite thin. A few deep drill holes into oceanic crust have intercepted gabbro, but it is not layered like ophiolite gabbro.

Beyond issues of layer thicknesses mentioned above, a problem arises concerning compositional differences of silica (SiO_2) and titania (TiO_2). Ophiolite basalt contents place them in the domain of subduction zones (~55% silica, <1% TiO_2), whereas mid-ocean ridge basalts typically have ~50% silica and 1.5–2.5% TiO_2. These chemical differences extend to a range of trace elements as well (that is, chemical elements occurring in amounts of 1000 ppm or less).

Additionally, the crystallization order of feldspar and pyroxene (clino- and orthopyroxene) in the gabbros is reversed, and ophiolites also appear to have a multi-phase magmatic complexity on par with subduction zones. Indeed, there is increasing evidence that most ophiolites are generated when subduction begins and thus represent fragments of fore-arc lithosphere. This led to introduction of the term "supra-subduction zone" (SSZ) ophiolite in the 1980s to acknowledge that some ophiolites are more closely related to island arcs than ocean ridges. Consequently, some of the classic ophiolite occurrences thought of as being related to seafloor spreading (Troodos in Cyprus, Semail in Oman) were found to be "SSZ" ophiolites, formed by rapid extension of fore-arc crust during subduction initiation.

A fore-arc setting for most ophiolites also solves the otherwise-perplexing problem of how oceanic lithosphere can be emplaced on top of continental crust. It appears that continental accretion sediments, if carried by the down going plate into a subduction zone, will jam it up and cause subduction to cease, resulting in the rebound of the accretionary prism with fore-arc lithosphere (ophiolite) on top of it. Ophiolites with compositions comparable with hotspot-type eruptive settings or normal mid-oceanic ridge basalt are rare, and those examples are generally strongly dismembered in subduction zone accretionary complexes *[Wikipedia]*.

Pegmatites

GEOLOGY Base

https://geologybase.com/pegmatites/

Pegmatites are intrusive or plutonic igneous rocks with wholly crystalline, unusually large, or coarse crystals that may sometimes interlock. These rocks form from a low-viscosity fluid phase rich in volatile compounds formed during the crystallization of the last magma portion. Usually, pegmatitic rocks will have crystals that are at least 1 cm in diameter, with the larger ones more than 3 cm and some as large as 10 m. Pegmatite crystals may vary in size, but some pegmatites may be equigranular – have nearly equal crystal sizes. Also, they may be spatially zoned and directionally oriented.

Most pegmatites have quartz, feldspar, and mica, with a silicic composition similar to granites. However, this texture can be shown by mafic rocks like basalt, gabbro, syenite, etc. Pegmatite or pegmatitic texture only describes the texture, not the mineral composition. Therefore, we may use the rock name as a prefix to indicate the mineral composition. For instance, granite pegmatite, diorite pegmatite, or gabbro pegmatite suggest that the said rock has granite, diorite, and gabbro composition, respectively. However, there is no unanimity on naming.

Pegmatite bodies are smaller than usual magma intrusions. Therefore, they are commonly found as small pockets, veins, dikes (including dike swarms), or lenses, especially at the margins of large intrusions and batholiths. Geographically, pegmatites occur anywhere in the world, and they are commonly found on cratons and greenschist-facies (Barrovian facies) metamorphic belts.

Since most pegmatites have a granitic composition, pegmatites are pinkish, gray, or whitish. However, you can find those that are colorless or darker (dark gray or black) if they have mafic minerals. Also, depending on the unique mineralogy, you will find some with red, brown, green, or other colors.

Mineral composition

Most simple pegmatite will have mainly granite to granodiorite composition. Such rocks will mostly have large crystals of feldspar, quartz, and mica (like lepidolite, biotite or muscovite). Also, they may have any other minerals associated with granitic rocks like aplite. However, some will have nepheline syenite composition. It is like granitic with quartz replaced with nepheline, a feldspathoid. And in rare cases, you may have pegmatite with intermediate to mafic rock composition.

Most complex pegmatites have a composition like granite but are enriched with some incompatible elements and minerals not typically found in most igneous rocks. Some may also be of intermediate to mafic composition. Incompatible elements are those with a too-large or small atomic number or very high or low ionic charge or size. So they cannot participate in the rock formation. Instead, they will remain dissolved in water and eventually form their minerals. Examples of incompatible elements in pegmatites are uranium (U), niobium (Nb), boron (B), yttrium (Y), phosphorus (P), fluorine (F), lithium (Li), zirconium (Zr) and beryllium (Be). Others are Strontium (Sr), Barium (Ba), scandium (Sc), Tantalum (Ta), thorium (Th), cesium (Cs), Tin (Sn), Titanium (Ti), Bismuth (Bi), and some Rare Earth Minerals (REEs).

These incompatible elements may form minerals such as pollucite (Cs), spodumene (Li), Beryl (Be), tantalite-columbite (Ta, and Nb), tourmaline (Li, B), cassiterite (Sn). Also, complex pegmatites may also have beryl, lepidolite, topaz, apatite, garnet, emerald, spodumene, tourmaline, mica, monazite, and fluorite. Other minerals are amblygonite, triphylite, molybdenite, scapolite, columbite etc. These minerals are not typical in ordinary igneous rocks. Lastly, the large crystal size of some pegmatitic rocks makes it hard to determine mineral composition accurately.

Formation of pegmatites

At the initial stages following a significant magma intrusion, minerals with higher melting points will start crystallizing and slowly be depleted from the magma. As the process continues, the remaining magma is increasingly enriched with minerals with lower melting point as well as with, water, and volatiles. These volatile compounds include carbon dioxide, boron, fluorine, chlorine, and phosphorus. Also, any incompatible minerals or elements will remain in this melt, specifically in water. At the final stage of magma crystallization, the exceptionally high amount of dissolved water causes a *phase separation*. So, that ultimately a last magma melt phase and a fluid phase or superheated water phase rich in silica, alkalis, volatiles, and incompatible trace elements develops. The fluid phase is what forms pegmatites. The presence of volatiles, i.e., water, carbon dioxide, chlorine, and fluorine, will tremendously lower the viscosity of the fluid phase (hydrous fluid). So, ions or molecules can move, migrate, or diffuse quickly to the crystal growth site. Also, the crystal growth rate (ions or molecules joining a growing crystal) exceeds nucleation (formation of new nuclei or sites for crystallization). Otherwise, the pegmatites would have many much smaller crystals.

Lastly, pegmatite formation does not have to be associated with intrusive rocks or magma. Such cases may be from melting or anatexis of metamorphic rock under high pressure and temperature. The melting will make fluids, volatiles, and trace elements sweat out, forming a fluid phase pocket seen in felsic gneiss.

Emeralds (green), schorl tourmaline (black), and garnet (pinkish-reddish) in quartz (medium-brown glassy) and feldspar (grayish) Crabtree Pegmatite from Devonian of North Carolina, USA. Photo credit: James St. John, Wikimedia, CC BY 2.0.

Graphic granite from Devonian of New Hampshire, USA with interlocking quartz (dark gray) and potassium feldspar (whitish). Photo credit: James St. John, Wikimedia, CC BY 2.0.

Partial Melting and Fractional Crystallization

https://opengeology.org/petrology/03-magma/

See also Appendix of My GeoGuide No. 22: Uppermost Nappes of the Asterousia Mts - Coast Road Kali Limenes to Chrysostoms

Incomplete Melting

Melting can only occur if temperature exceeds the solidus, and temperatures rarely, if ever, reach the liquidus. Because the geothermal gradient is different in different places, this means that partial melting occurs but does not occur everywhere. So, magmas generally form by melting of an originally solid *parent rock* that does not melt completely. When a rock melts only partially, producing a melt that contains melted low-temperature minerals and leaving behind solid high-temperature minerals, we call the process *anatexis*. In the mantle, for example, anatexis of ultramafic rock produces basalts.

3.34 Metasedimentary migmatite

Migmatites (from the Greek *migma* meaning *mixture*, and *ite*, referring to *rock*) are rocks composed of two different components that are mixed, or swirled, together. Typically migmatites contain a light colored segregation that in many cases appears to have formed by partial melting of the darker surrounding material. In the crust, many migmatites, such as the one seen in Figure 3.34, are thought to have formed by anatexis associated with metamorphism of a parental sedimentary rock. The result is a mixed rock that contains both metamorphic and igneous components. The melt that develops eventually cools and crystallizes just like any other magma does, and will sometimes contain large crystals (phenocrysts) after completely solidified. If the melt migrates away from where it was produced, identifying its origin may become problematic, and the residual material left behind will not resemble the original sedimentary parent. It seems apparent, nonetheless, that large scale anatexis of crustal rocks can produce large volumes of granitic melts that later form granitic plutons. The plutons may contain xenoliths (included unmelted pieces) of the original rock that melted to form the granitic magma.

Equilibrium or Not?

In an equilibrium melting process, the melt and solid remain in contact and in chemical equilibrium as melting occurs. The system is “closed” – the overall composition does not change – so the melt and remaining solid material add up to the starting composition. Consider the melting process that may occur when a rock is heated. Melting begins at the solidus temperature, and the first melt is formed by the melting of low-temperature minerals, singly or in combination. The rest of the minerals remain unmelted. Melting progresses as temperature increases, and different minerals melt at different temperatures.

As the amount of melting increases, the melt composition evolves to be more like its original parent rock until everything has melted. During this process, the minerals present will change, and the compositions of solid solution mineral crystals will change as atoms migrate in and out of the solid crystals. It does not matter if the rock melts partially or completely; if melt and solids continue to react, chemical equilibrium is possible as compositions change in response to temperature changes. The same concept of equilibrium applies to crystallization. If equilibrium is maintained during crystallization, crystals will be homogeneous in composition and will change proportions and compositions systematically as temperature decreases. However, disequilibrium can occur if the migration of atoms through the solid crystals, or through a viscous melt, is not fast enough to keep up with cooling.

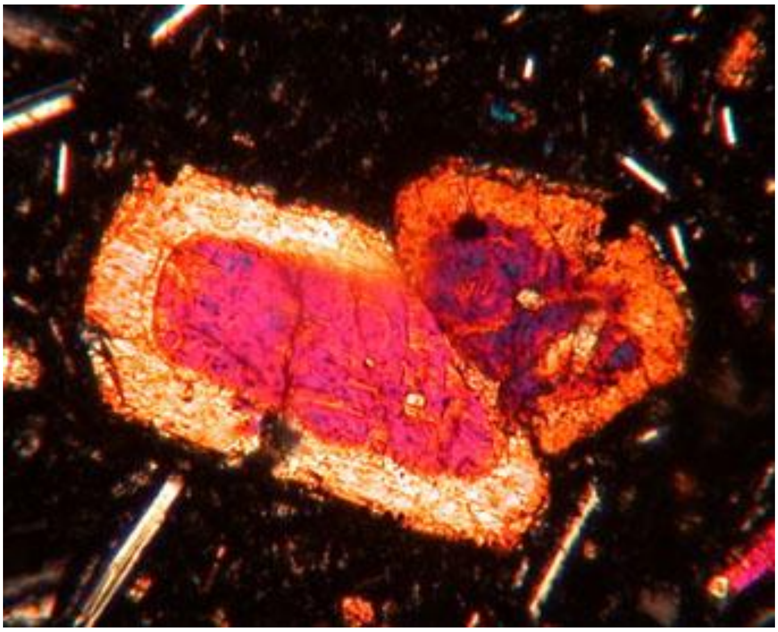

3.35 A zoned clinopyroxene crystal in a basalt

When studying rocks, petrologists may find it difficult to decide if crystals and melt stayed in equilibrium. Some volcanic rocks, however, contain zoned crystals that are evidence of disequilibrium. Figure 3.35 shows a polarizing microscope view of a large compositionally zoned grain of clinopyroxene in a basalt. The dark material surrounding the clinopyroxene is mostly volcanic glass, and the needle-shaped light colored crystals are plagioclase. If the clinopyroxene grain was homogeneous, the colors induced by the polarizers would be the same in all parts of the grain. Zoning of this sort is evidence that the melt and crystals did not stay in equilibrium during crystallization. The center of the crystal grew at high temperature, and as temperature decreased the crystals grew larger. If the minerals and melt stayed in equilibrium, the grain (no matter the size) would have a homogeneous composition. But in zoned crystals the crystal cores have compositions formed at higher temperature than the rims did. The outer zones have compositions that formed at lower temperature because atoms could not migrate into and through the crystals fast enough to maintain compositional homogeneity. Thus, only partial equilibrium was maintained. Many volcanic mineral crystals have broad homogeneous centers but are zoned near their rims, suggesting that they stayed in equilibrium with the melt until the latest stages of crystallization.

Partial Melting

Large scale disequilibrium melting occurs if a melt and a solid do not continue to react together, but instead become chemically isolated due to physical separation. For example, if a rock melts partially and the magma escapes upwards, the melt and remaining solid material cannot react to stay in chemical equilibrium.

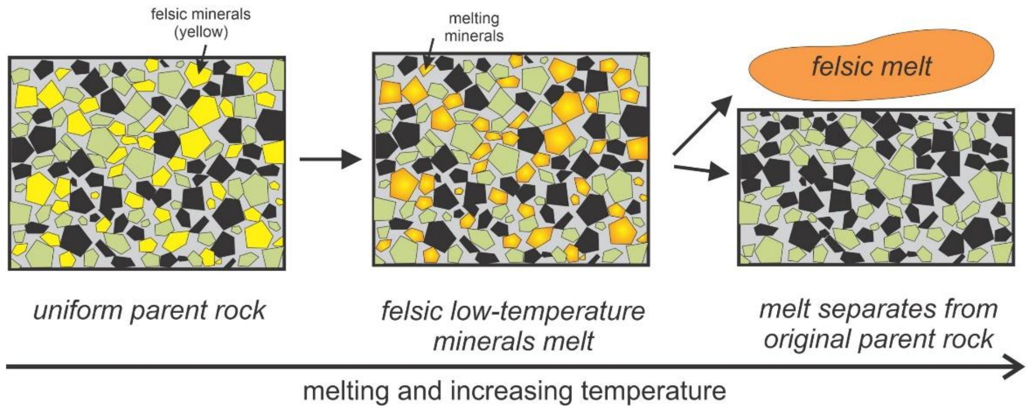

3.36 Partial melting

Figure 3.36 shows melting of an original parent rock that contains several different minerals. The first minerals to melt are (generally Si-rich) low-temperature minerals (shown in yellow). So, initial melting produces a relatively silicic magma (shown in orange). This melt may subsequently become separated from the leftovers of the original rock. Consequently, a melt of different composition from the parent has been produced and may move upwards in Earth.

Partial melting is a widespread and important process that occurs in the source region for most magmas. Low-temperature minerals always melt first, either individually or in consort with others. They are relatively silica-rich minerals compared with others in a rock, so when partial melting occurs, the melts are more silicic than the parent rock is. The remaining rock becomes depleted in silicic components and, therefore, more mafic than its parent. When this happens, silicic melts migrate upwards, leaving more mafic residue behind. So, partial melting explains, in part, why the Earth has differentiated into a more silicic crust and more mafic mantle during its 4.6 Ma year lifetime. These generalizations always apply, but the specific products of partial melting depend on the starting material composition and the amount of melting. Furthermore, the results will be different if the parent rock is already depleted.

Earth's mantle is ultramafic; if it melted completely it would produce ultramafic magma, but, as discussed previously, complete melting cannot occur because there is no known mechanism for heating the mantle to the very high temperatures needed to melt it completely. Partial melting, however, is common, and the upper mantle is the source of many magmas that move within the crust and sometimes reach the surface. Because the upper mantle has a relatively uniform composition, partial melting of mantle produces similar magmas worldwide, almost all mafic, equivalent to basalt compositions. More silicic magmas may also be generated in the mantle, but they are uncommon. Similarly, partial melting of subducted ocean crust, which is basaltic everywhere, generally produces magmas of intermediate composition, and partial melting of lower continental crust produces silicic magmas (equivalent to granite).

Fractional Crystallization

Fractional crystallization, the opposite of partial melting, occurs when a magma partially crystallizes and the remaining magma becomes segregated from the crystals. In these circumstances, the new *evolved magma* will have a different composition from its *parental magma*. The evolved magma, which is more silicic than its parent was, may move upwards, leaving the high-temperature (mafic) minerals behind. Fractional crystallization, like partial melting, has been a key process contributing to differentiation of Earth.

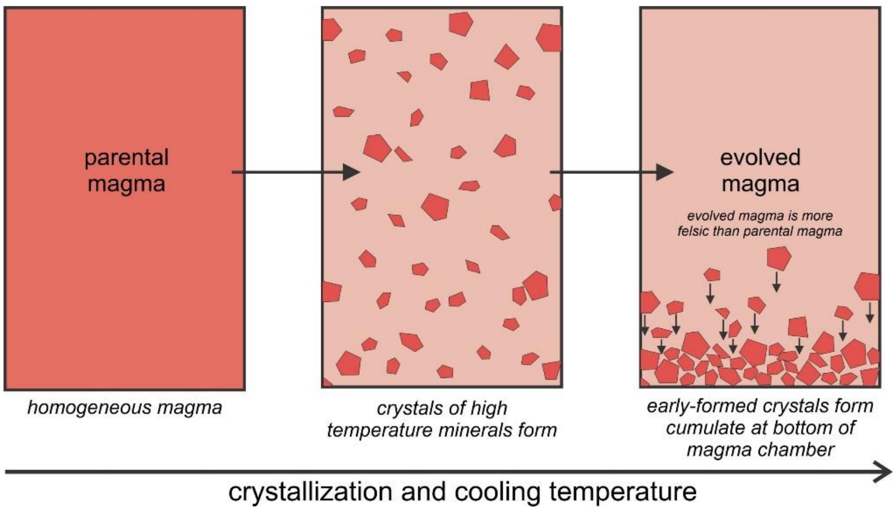

3.37 Diagram showing fractional crystallization

Fractional crystallization may occur when newly formed crystals sink to the bottom of a magma chamber and no longer stay in equilibrium with the melt. Figure 3.37, a schematic diagram, shows the principles involved. While cooling, a parental magma crystallizes some high temperature minerals. These minerals eventually sink to the bottom of the magma chamber, leaving an evolved magma above. Because high-temperature minerals are mafic, the evolved melt is more silicic (less mafic) than the original parent magma. During this process, a *cumulate* rock forms at the bottom of the magma chamber, and the evolved magma may move upwards and become completely separated from the cumulate. Fractional crystallization explains the origins of cumulate rocks like the chromite cumulates.

Other Processes Explaining Variations in Magma Composition

Fractional crystallization is undoubtedly the most important process that changes magma composition after a magma forms. Other mechanisms, however, also lead to changes. For example, in some settings, hot magmas may melt surrounding rocks and assimilate them into the magma. Generally, we think of this *assimilation* occurring when mafic magmas encounter more silicic rocks, because mafic magmas may be hotter than the silicic rock's melting temperature is. So, assimilation can make magma more silicic and is most likely to occur in the (silicic) crust. Some volcanic rocks contain crustal xenoliths, inclusions of rock fragments incorporated as solid pieces into the melt; often the xenoliths show evidence of partial melting. It is no stretch to assume that sometimes xenoliths melt and mix in completely. Some geochemical data, too, supports the idea that crustal material has been incorporated into a mantle-derived melt.

Different magmas may also combine to produce hybrid magmas of different compositions. However, *magma mixing* is unlikely to happen if magma compositions are too different because different magmas have different melting temperatures, densities, and viscosities. Although some evidence suggests that magma mixing occurs on a small scale, most petrologists believe it is generally a minor contributor to magma diversity. A third process, *liquid immiscibility*, has also been proposed as a process that may lead to change in magma composition. Immiscible liquids unmix in much the same way that chicken soup separates into broth and fat upon cooling. Experimental evidence suggests, for instance, that sometimes a sulfide-rich melt may unmix from mafic silicate magma – a potential important process forming ore deposits, or that alkali-rich magmas may unmix from less alkaline ones. Some petrologists have invoked this last process to explain the origin of *carbonatites*, that are unusual carbonate-rich magmas.

Parental Magmas and Differentiation

Only a few rare magmas may not be evolved. For example, the white veins (termed *leucosomes*) in migmatites that form by partial melting of sedimentary rocks may not have changed composition after they formed (Figure 3.34). The leucosomes appear to have been created by partial melting of metasedimentary rock, and the melt has remained local and has not differentiated.

The majority of magmas, however, evolve from some parental magma. They are evolved melts, not melts having the composition created during initial melting. Subsequently, as crystallization progresses, magma compositions follow what is called a *liquid line of descent*, producing a series of magmas of different compositions as fractional crystallization removes specific minerals from the melt.

If solid mantle melted directly, either partially or completely, to create magma, the magma would be called a *primary magma*. Primary magmas have undergone no differentiation and have the same composition they started with. Specifically, if they come from the ultramafic mantle, and were not subsequently modified, they must have a very high Mg:Fe ratio and be enriched in Cr and Ni just like mantle rocks, and petrologists use these and other characteristics to test if magmas could be primary magmas. Most magmas fail the tests, and primary magmas are exceptionally rare, or may not exist at all. Some magmas and rocks, however, come close to being primary, and petrologists describe them as *primitive*, meaning they have undergone only minor differentiation.

Parental magmas may be primary or primitive. The only requirement is that they lead to magmas of other compositions. If a collection of melts with different compositions evolve from the same parent, they form a *magma series*. Although the melts have different compositions, they will share some chemical characteristics, especially trace element compositions and isotopic ratios. A challenge for petrologists is to study the compositions of an inferred magma series to learn the composition and source of the original parent.

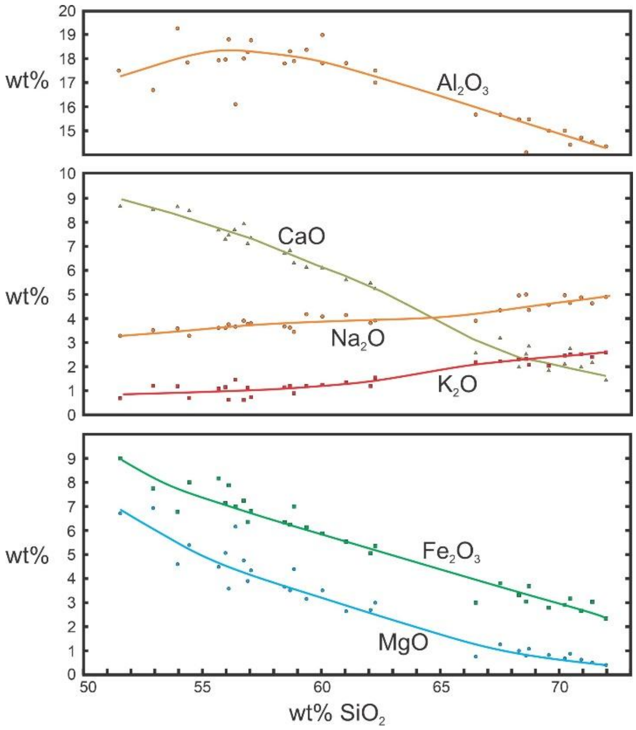

3.40 Harker diagram for volcanic rocks of the Crater Lake region, Oregon

Typically, petrologists begin their quest by obtaining analyses of the rocks and plotting the results on different kinds of *composition diagrams*. For example, *Harker diagrams*, first used in 1902, have SiO_2 content as the horizontal axis and other oxides plotted vertically (Figure 3.40). SiO_2 is chosen as the abscissa because it generally shows the most variation of all oxides, and because it relates closely with magma temperature and the amount of fractional crystallization.

When looking at Harker diagrams, the principles are that (1) if derived from a common parent, rock compositions should trend smoothly across a diagram; and (2) the most mafic composition is closest to the parent magma composition. So, if a Harker diagram reveals smooth trends, it is possible that all the magmas derived from the same parent and that the low SiO_2 end of the graphs are closest to the magma's parent composition. Harker diagrams are only one kind of composition diagram; many others with different oxides on the axes are commonly used.

Figure 3.40 shows a well-studied Harker diagram for volcanic rocks from near Crater Lake, Oregon, based on the data of Howell Williams (1942). Each point represents a different volcanic rock from the same region; the horizontal axis shows the SiO_2 content of the rock and the vertical axis the amount of other oxides present. The solid lines show the smoothed trends. The smooth trends are evidence that the different rocks may have derived from the same original parental magma. The Crater Lake magmas range from *basalt* (on the left side of the diagram) to *rhyolite* (on the right side). Based on the trends shown, Williams concluded that the magmas all came from a common parent magma and that they evolved by fractional crystallization. The basalt composition is closest to that parent.

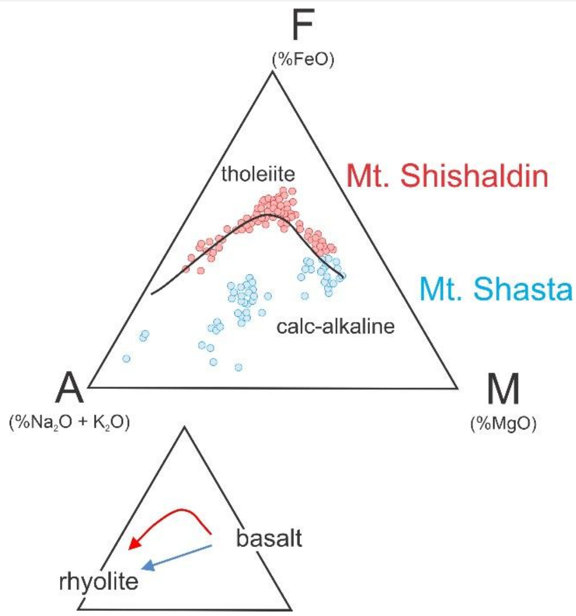

3.41 AFM diagrams for rocks from Mt. Shishaldin, Alaska, and from Mt. Shasta, California

A second commonly used way to look at magma composition is to plot compositions on an AFM diagram (Figure 3.41). AFM diagrams ignore SiO_2 and instead look at alkali (Na_2O + K_2O), iron as FeO (assuming it is not Fe_2O_3), and MgO content. The triangle corners are: A = alkali oxide weight %, F = FeO weight %, and M = MgO weight %. Many studies have found that magma series follow one of two trends, the *tholeiite* trend or the *calc-alkaline* trend, and we easily see these on an AFM diagram. Figure 3.41 is an AFM diagram comparing rocks from Shishaldin Volcano (Aleutian Islands) and Shasta Volcano (California). Each point represents an analysis of an individual rock. Shishaldin is an island arc volcano associated with an oceanic plate subducting under another oceanic plate. Shasta is a continental margin volcano where an oceanic plate is subducting under a continental plate. The Shishaldin data follow a tholeiite trend, depicted by the solid line and red arrow that initially moves toward the F-corner before curving downward toward the A-corner. The Shasta data follow a calc-alkaline trend (depicted by the blue line that heads directly toward the A-corner).

Whether tholeiitic or calc-alkaline, originally mafic magmas can produce rocks ranging from basalt to rhyolite, as the bottom triangle in Figure 3.41 shows. At both Shishaldin and Shasta Volcanos, more primitive parental magmas were mafic and the later evolved magmas were silicic. They differ, however, because tholeiitic magmas become iron-rich as they evolve, moving initially toward the F apex of the triangle. Calc-alkaline trends go directly from basalt to rhyolite.

The trends on an AFM diagram reveal clues about the environments in which the magmas differentiated. The difference between calc-alkaline and tholeiite trends is due to the oxidation state of iron. If iron is mostly oxidized, magnetite (Fe_3O_4), a mineral that contains oxidized iron (Fe^{3+}), crystallizes early from a melt. If the iron is mostly reduced (existing as Fe^{2+}), magnetite does not crystallize. In calc-alkaline magmas, the iron is oxidized, leading to crystallization of magnetite. Consequently, when mafic minerals crystallize, iron is removed from the magma as fast as magnesium and the melt's Fe:Mg ratio remains about constant during differentiation. In tholeiitic magmas, olivine and pyroxene crystallize first and magnetite may not crystallize at all. Olivine and pyroxene have high Mg/Fe ratios compared with melt, and the magma becomes enriched in iron during the initial stages of crystallization. Calc-alkaline magmas are dominant in *andesitic-type* subduction zones, such as California's Cascade Mountains. Mt. Shasta is an example. Tholeiitic trends occur mostly in island arcs, such as the Aleutian Islands, and Shishaldin Volcano is an example.

Fission track dating

https://en.wikipedia.org/wiki/Fission_track_dating

Method

Unlike other isotopic dating methods, the "daughter" in fission track dating is an effect in the crystal rather than a daughter isotope. Uranium-238 undergoes spontaneous fission decay at a known rate, and it is the only isotope with a decay rate that is relevant to the significant production of natural fission tracks; other isotopes have fission decay rates too slow to be of consequence. The fragments emitted by this fission process leave trails of damage (fossil tracks or ion tracks) in the crystal structure of the mineral that contains the uranium. The process of track production is essentially the same by which swift heavy ions produce ion tracks. Chemical etching of polished internal surfaces of these minerals reveals spontaneous fission tracks, and the track density can be determined. Because etched tracks are relatively large (in the range 1 to 15 micrometres), counting can be done by optical microscopy, although other imaging techniques are used. The density of fossil tracks correlates with the cooling age of the sample and with uranium content, which needs to be determined independently.

To determine the uranium content, several methods have been used. One method is by neutron irradiation, where the sample is irradiated with thermal neutrons in a nuclear reactor, with an external detector, such as mica, affixed to the grain surface. The neutron irradiation induces fission of uranium-235 in the sample, and the resulting induced tracks are used to determine the uranium content of the sample because the 235U:238U ratio is well known and assumed constant in nature. However, it is not always constant. To determine the number of induced fission events that occurred during neutron irradiation an external detector is attached to the sample and both sample and detector are simultaneously irradiated by thermal neutrons. The external detector is typically a low-uranium mica flake, but plastics such as CR-39 have also been used. The resulting induced fission of the uranium-235 in the sample creates induced tracks in the overlying external detector, which are later revealed by chemical etching. The ratio of spontaneous to induced tracks is proportional to the age.

Another method of determining uranium concentration is through LA-ICPMS, a technique where the crystal is hit with a laser beam and ablated, and then the material is passed through a mass spectrometer.

Applications

Unlike many other dating techniques, fission-track dating is uniquely suited for determining low-temperature thermal events using common accessory minerals over a very wide geological range (typically 0.1 Ma to 2000 Ma). Apatite, sphene, zircon, micas and volcanic glass typically contain enough uranium to be useful in dating samples of relatively young age (Mesozoic and Cenozoic) and are the materials most useful for this technique. Additionally low-uranium epidotes and garnets may be used for very old samples (Paleozoic to Precambrian). The fission-track dating technique is widely used in understanding the thermal evolution of the upper crust, especially in mountain belts. Fission tracks are preserved in a crystal when the ambient temperature of the rock falls below the annealing temperature. This annealing temperature varies from mineral to mineral and is the basis for determining low-temperature vs. time histories. While the details of closure temperatures are complicated, they are approximately 70 to 110 °C for typical apatite, c. 230 to 250 °C for zircon, and c. 300 °C for titanite.

Because heating of a sample above the annealing temperature causes the fission damage to heal or anneal, the technique is useful for dating the most recent cooling event in the history of the sample. This resetting of the clock can be used to investigate the thermal history of basin sediments, kilometer-scale exhumation caused by tectonism and erosion, low temperature metamorphic events, and geothermal vein formation. The fission track method has also been used to date archaeological sites and artifacts. It was used to confirm the potassium-argon dates for the deposits at Olduvai Gorge.

Provenance analysis of detrital grains

A number of datable minerals occur as common detrital grains in sandstones, and if the strata have not been buried too deeply, these minerals grains retain information about the source rock. Fission track analysis of these minerals provides information about the thermal evolution of the source rocks and therefore can be used to understand provenance and the evolution of mountain belts that shed the sediment. This technique of detrital analysis is most commonly applied to zircon because it is very common and robust in the sedimentary system, and in addition it has a relatively high annealing temperature so that in many sedimentary basins the crystals are not reset by later heating.

Fission-track dating of detrital zircon is a widely applied analytical tool used to understand the tectonic evolution of source terrains that have left a long and continuous erosional record in adjacent basin strata. Early studies focused on using the cooling ages in detrital zircon from stratigraphic sequences to document the timing and rate of erosion of rocks in adjacent orogenic belts (mountain ranges). A number of recent studies have combined U/Pb and/or Helium dating (U+Th/He) on single crystals to document the specific history of individual crystals. This double-dating approach is an extremely powerful provenance tool because a nearly complete crystal history can be obtained, and therefore researchers can pinpoint specific source areas with distinct geologic histories with relative certainty. Fission-track ages on detrital zircon can be as young as 1 Ma to as old as 2000 Ma.